The molecular bases of δ/αβ T cell–mediated antigen recognition

Daniel G. Pellicci,[1,2]* Adam P. Uldrich,[1,2]* Jérôme Le Nours,[3,4] Fiona Ross,[1,2] Eric Chabrol,[3] Sidonia B.G. Eckle,[1] Renate de Boer,[5] Ricky T. Lim,[1] Kirsty McPherson,[1] Gurdyal Besra,[6] Amy R. Howell,[7] Lorenzo Moretta,[8] James McCluskey,[1] Mirjam H.M. Heemskerk,[5] Stephanie Gras,[3,4] Jamie Rossjohn,[3,4,9]** and Dale I. Godfrey[1,2]**

[1]Department of Microbiology and Immunology, Peter Doherty Institute for Infection and Immunity and [2]Australian Research Council Centre of Excellence in Advanced Molecular Imaging, University of Melbourne, Parkville, Victoria 3010, Australia
[3]Department of Biochemistry and Molecular Biology, School of Biomedical Sciences and [4]Australian Research Council Centre of Excellence in Advanced Molecular Imaging, Monash University, Clayton, Victoria 3800, Australia
[5]Department of Hematology, Leiden University Medical Center, 2300 RC Leiden, Netherlands
[6]School of Biosciences, University of Birmingham, Edgbaston, Birmingham B15 2TT, England, UK
[7]Department of Chemistry, University of Connecticut, Storrs, CT 06269
[8]Istituto Giannina Gaslini, 16147 Genova, Italy
[9]Institute of Infection and Immunity, School of Medicine, Cardiff University, Heath Park, Cardiff CF14 4XN, Wales, UK

αβ and γδ T cells are disparate T cell lineages that can respond to distinct antigens (Ags) via the use of the αβ and γδ T cell Ag receptors (TCRs), respectively. Here we characterize a population of human T cells, which we term δ/αβ T cells, expressing TCRs comprised of a TCR-δ variable gene (Vδ1) fused to joining α and constant α domains, paired with an array of TCR-β chains. We demonstrate that these cells, which represent ∼50% of all Vδ1$^+$ human T cells, can recognize peptide- and lipid-based Ags presented by human leukocyte antigen (HLA) and CD1d, respectively. Similar to type I natural killer T (NKT) cells, CD1d–lipid Ag–reactive δ/αβ T cells recognized α-galactosylceramide (α-GalCer); however, their fine specificity for other lipid Ags presented by CD1d, such as α-glucosylceramide, was distinct from type I NKT cells. Thus, δ/αβTCRs contribute new patterns of Ag specificity to the human immune system. Furthermore, we provide the molecular bases of how δ/αβTCRs bind to their targets, with the Vδ1-encoded region providing a major contribution to δ/αβTCR binding. Our findings highlight how components from αβ and γδTCR gene loci can recombine to confer Ag specificity, thus expanding our understanding of T cell biology and TCR diversity.

CORRESPONDENCE
Jamie Rossjohn:
jamie.rossjohn@monash.edu
OR
Dale I. Godfrey:
godfrey@unimelb.edu.au

Abbreviations used: Ag, antigen; α-GalCer, α-galactosylceramide; α-GlcCer, α-glucosylceramide; BSA, buried surface area; CDR, complementarity-determining region; MAIT cell, mucosal-associated invariant T cell; rmsd, root-mean-square deviation; SPR, surface plasmon resonance.

αβ and γδ T cells, which express highly polymorphic TCRs on their surface, play a vital role in immunity. In humans, the majority of T cells use TCRs derived from the α and β TCR gene loci, whereupon the αβTCR architecture is composed of the variable (Vα), joining (Jα), and constant (Cα) gene segments that form the TCR-α chain, whereas the Vβ, Dβ (diversity), Jβ, and Cβ gene segments constitute the TCR-β chain (Turner et al., 2006). Multiple TCR genes within the α and β loci, coupled with random nucleotide (N) additions at V-(N)-J, V-(N)-D, and D-(N)-J junctional regions, underpin the vast αβTCR repertoire (Turner et al., 2006). This diversity is manifested within the Vα and Vβ domains, each of which contains three complementarity-determining regions (CDRs), collectively forming the antigen (Ag) recognition site of the αβTCR. The αβ T cell diversity provides the capability of αβTCRs to recognize a range of antigenic determinants presented by polymorphic and monomorphic Ag-presenting molecules (Godfrey et al., 2008; Bhati et al., 2014).

αβTCRs are typically considered to recognize short peptide (p) fragments bound within

*D.G. Pellicci and A.P. Uldrich contributed equally to this paper.
**J. Rossjohn and D.I. Godfrey contributed equally to this paper.

© 2014 Pellicci et al. This article is distributed under the terms of an Attribution–Noncommercial–Share Alike–No Mirror Sites license for the first six months after the publication date (see http://www.rupress.org/terms). After six months it is available under a Creative Commons License (Attribution–Noncommercial–Share Alike 3.0 Unported license, as described at http://creativecommons.org/licenses/by-nc-sa/3.0/).

The Rockefeller University Press $30.00
J. Exp. Med. 2014 Vol. 211 No. 13 2599–2615
www.jem.org/cgi/doi/10.1084/jem.20141764

The Journal of Experimental Medicine

Downloaded from http://rupress.org/jem/article-pdf/211/13/2599/1749468/jem_20141764.pdf by guest on 08 February 2026

the Ag-binding cleft of molecules encoded by the polymorphic MHC. Here, the αβTCR accommodates a wide range of pMHC landscapes with a polarized and approximately conserved docking mode, whereby the Vα and Vβ domains are positioned over the α2 and α1 helices of MHC-I, respectively (Gras et al., 2012). Alternately, some αβ T cells are activated by lipid-based Ags presented by MHC-I–like molecules belonging to the CD1 family (Brigl and Brenner, 2004). The CD1d system, which presents lipid Ags to type I and type II NKT cells, is the best understood in terms of lipid Ag recognition (Girardi and Zajonc, 2012; Rossjohn et al., 2012). Here, a semi-invariant NKT TCR (Vα24-Jα18 in humans), which typifies type I NKT cells, binds a wide range of chemically distinct ligands in a conserved docking mode, whereby the TCR sits in a parallel manner above the F′ pocket of CD1d (Rossjohn et al., 2012). As such, the NKT TCR has been likened to an innate-like pattern recognition receptor (Scott-Browne et al., 2007). In contrast, type II NKT cells can adopt differing docking strategies in binding to CD1d-restricted lipid-based ligands and exhibit features that more closely resemble that of αβTCR recognition in adaptive immunity (Girardi et al., 2012; Patel et al., 2012; Rossjohn et al., 2012). It has also recently been established that mucosal-associated invariant T cells (MAIT cells), which express a semi-invariant αβTCR, recognize vitamin B–based metabolites presented by the monomorphic MHC-I–related protein (MR1; Kjer-Nielsen et al., 2012; Corbett et al., 2014). Here, the MAIT TCR draws upon features typified by innate and adaptive immunity in recognizing these small molecule metabolites (Patel et al., 2013; Eckle et al., 2014). Accordingly, the αβTCR lineage shows remarkable versatility in recognizing three distinct classes of ligands (Bhati et al., 2014).

The γδ T cell lineage uses γδTCRs that are derived from the γ and δ TCR gene loci (O'Brien et al., 2007; Vantourout and Hayday, 2013). γδ T cells and αβ T cells develop from common intrathymic precursors but branch into separate lineages at the time when they undergo TCR gene rearrangement and differentiation (Xiong and Raulet, 2007; Ciofani and Zúñiga-Pflücker, 2010). γδ T cells rearrange Vγ and Jγ genes that join to the γ constant (Cγ) gene to form the TCR-γ chain, whereas rearrangement of Vδ, Dδ, and Jδ genes join to the δ constant (Cδ) gene to form the TCR-δ chain. Similar to αβTCRs, γδTCRs possess six CDR loops, three from each chain, which mediate Ag recognition (Bhati et al., 2014). The number of Vγ and Vδ genes in humans is relatively low (8× Vδ and 6× Vγ genes), and further limitation in repertoire diversity comes from restricted pairing of particular Vδ and Vγ genes. However, the potential to use the three Dδ genes, even in multiple copies, combined with N region modifications, dramatically increases TCR-δ diversity (O'Brien et al., 2007; Born et al., 2013). In contrast to αβ T cells, in which Vα and Vβ TCR chains are generally very diverse, some Vγ and Vδ TCR chains show tissue-specific and functional biases. For example, $V\delta2^+$ γδ T cells tend to produce inflammatory cytokines such as IFN-γ and TNF, predominate in human blood, and migrate to sites of inflammation, whereas $V\delta1^+$ γδ T cells tend to produce regulatory cytokines such as IL-10 and home to noninflamed tissues such as spleen and gut (O'Brien et al., 2007). Compared with αβ T cells, much less is known about what types of Ags are recognized by γδ T cells, although it is generally accepted that γδTCRs confer different specificity and functional characteristics (Vantourout and Hayday, 2013). Some γδTCRs can recognize Ags directly, whereas other studies have demonstrated that γδTCRs can recognize cell surface and soluble protein and peptide Ags and microbial metabolites in the absence of classical Ag-presenting molecules (Born et al., 2013; Vavassori et al., 2013; Sandstrom et al., 2014). Some γδ T cells can respond to Ag-presenting molecules in a ligand-independent manner, such as the MHC-II molecule or the MHC class I–like molecules T10/T22 and endothelial protein C receptor (EPCR), whereas others can recognize lipid-based Ags presented by members of the CD1 family (Born et al., 2013). The molecular bases of γδTCR recognition of CD1d-lipid Ag complexes were recently reported (Luoma et al., 2013; Uldrich et al., 2013).

Thus, αβ T cells and γδ T cells act in concert, using distinct TCRs to survey a wide range of Ags to enable protective immunity. Interestingly, the human Vδ gene locus is embedded within the Vα locus, and some human Vδ genes (Vδ4-Vδ8) encoded by TRDV 4, 5, 6, 7, and 8 are also referred to as Vα genes (Vα6, 21, 17, 28, and 14.1) encoded by TRAV 14, 23, 29, 36, and 38-2, respectively (Lefranc and Rabbitts, 1990), because these are capable of rearranging to either Dδ-Jδ-Cδ or Jα-Cα genes. Because these V genes can be used by both γδ and αβ T cell lineages, when paired with Cα, they are termed Vα genes, whereas they are termed Vδ genes when paired with Cδ (Lefranc and Rabbitts, 1990). However, the majority of human γδ T cells use the Vδ1, Vδ2, and Vδ3 variable regions, encoded by TRDV 1, 2, and 3 genes (O'Brien et al., 2007; Mangan et al., 2013). Although these do not have alternate TRAV names, these can also rearrange to Jα-Cα genes, and at least Vδ1 and Vδ3 can be expressed as a functional Vδ-Jα-Cα TCR chain that can pair with a functional TCR-β chain (Miossec et al., 1990; Peyrat et al., 1995). Here we describe a flow cytometry–based method for identifying $V\delta1^+$ $TCR\text{-}\beta^+$ cells, which we have termed δ/αβ T cells, based on their expression of TCRs comprising a TCR-δ variable gene 1 (Vδ1) joined to a TCR Jα and TCR Cα genes and paired with an array of TCR-β chains. These δ/αβ T cells were readily detectable in most humans and included cells with specificity for both peptide- and lipid-based Ags presented by MHC-I molecules and CD1d, respectively. We have determined the cell surface phenotype, Ag specificity, and functional capacity of a population of these cells. Using x-ray crystallography, we have elucidated the structural architecture of two δ/αβTCRs and show how these TCRs can recognize monomorphic and polymorphic Ag-presenting molecules via distinct mechanisms. Accordingly, we highlight a population of δ/αβ T cells that bind Ag by way of both Vδ and Vβ genes, thus reflecting a greater level of diversity and functional potential within the T cell lineage.

Downloaded from http://rupress.org/jem/article-pdf/211/13/2599/1749468/jem_20141764.pdf by guest on 08 February 2026

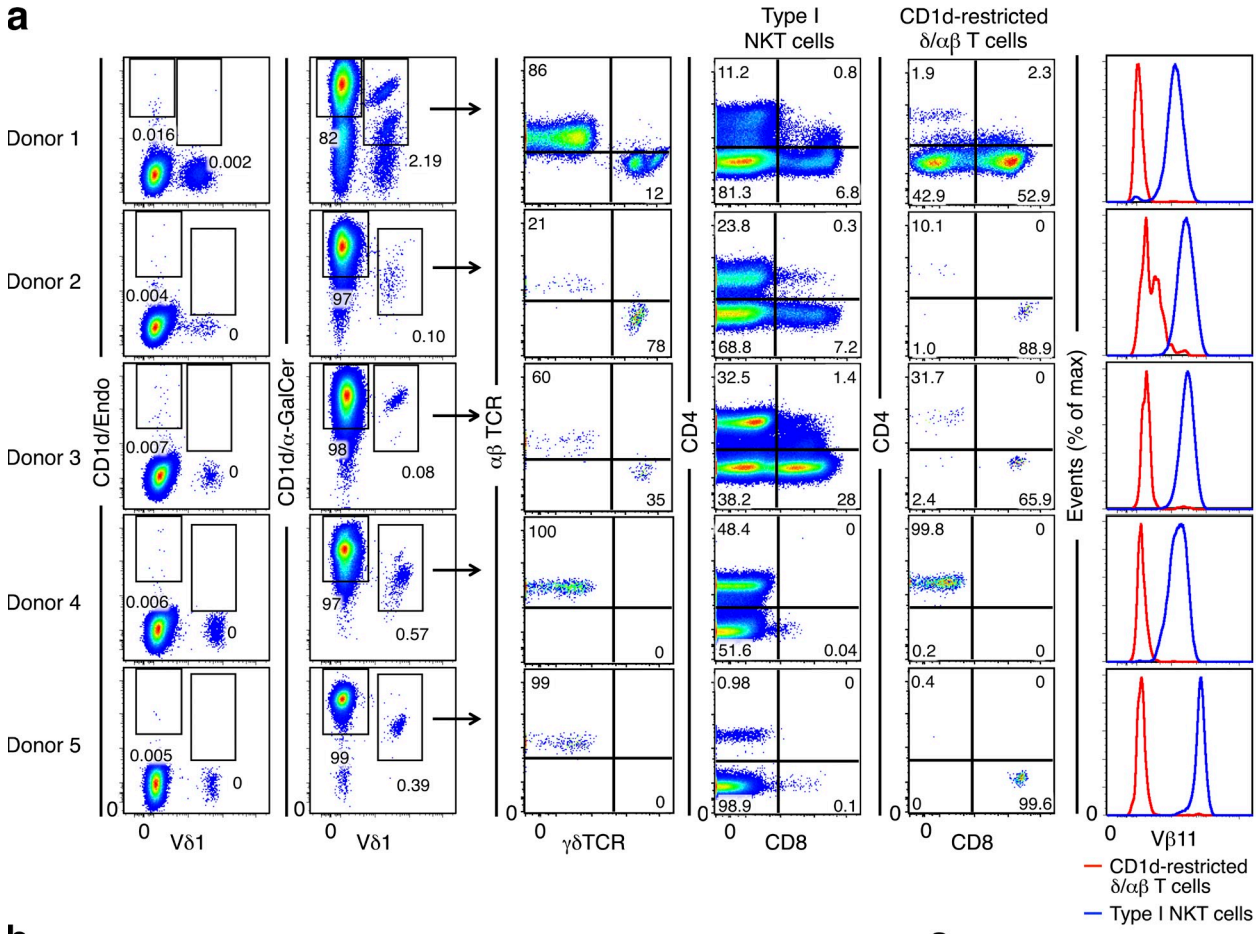

b

		TCRδ/α		TCRβ	
Sequence	Donor	Vδ-Jα	CDR3δ/α	Vβ-Jβ	CDR3β
1	1	Vδ1-Jα52	CALGVTGKLTF	Vβ2-Jβ1.1	CSAPGGVGAFF
2	2	Vδ1-Jα13	CALGDRPYSGGYQKVTF	Vβ13.3-Jβ1.1	CASSEGIVEGEAFF
3	3	Vδ1-Jα21	CALGEREVYNFNKFYF	Vβ12.3-Jβ1.4	CASTEGTNEKLFF
4	3	Vδ1-Jα9	CALGELGGGGFKTIF	Vβ1-Jβ2.1	CASSPRLAGVGEQFF
5	3	Vδ1-Jα31	CALGVPNRLMF	Vβ2-Jβ2	CSAQGGPTYNEQFF
6	4	Vδ1-Jα44	CALGELSGTASKLTF	Vβ2-Jβ2.1	CSARDPGAGPHEQFF
7	4	Vδ1-Jα10	CALGVITGGGNKLTF	Vβ9.1-Jβ2.3	CASNSGRTDTQYF
8	5	Vδ1-Jα34	CALGERSYNTDKLIF	Vβ2-Jβ1.5	CSARGIGQPVNQPQHF

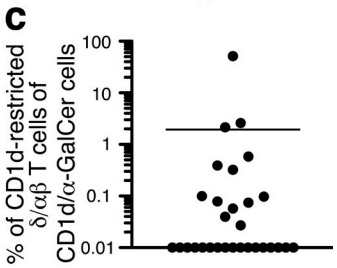

Figure 1. Identification of CD1d–α-GalCer tetramer–reactive Vδ1⁺ cells expressing a δ/αβTCR. (a) PBMCs from healthy donors were enriched for CD1d-α-GalCer⁺ cells, expanded in vitro, and analyzed by flow cytometry. CD3⁺ T cells were analyzed for Vδ1 (clone A13) versus CD1d-endogenous tetramer and CD1d–α-GalCer tetramer (left-hand density plots). CD3⁺ CD1d–α-GalCer tetramer⁺ Vδ1⁺ T cells were analyzed for αβTCR and γδTCR (middle density plots). CD3⁺ CD1d–α-GalCer tetramer⁺ γδTCR⁻ Vδ1⁻ "Type I NKT cells" and CD3⁺ CD1d–α-GalCer tetramer⁺ γδTCR⁻ Vδ1⁺ "CD1d-restricted δ/αβ T cells" were analyzed for CD4, CD8, and Vβ11 expression (right-hand plots). Data shown represent five healthy donors. (b) TCRs from CD3⁺ CD1d–α-GalCer tetramer⁺ Vδ1⁺ γδTCR⁻ cells derived from CD1d–α-GalCer tetramer–enriched and in vitro expanded PBMC samples were sequenced. Data shown are unique sequences, derived from five separate donors, performed across three separate experiments. (c) Percentage of CD1d-restricted δ/αβ T cells within the in vitro expanded CD1d–α-GalCer tetramer⁺ T cell population from 30 healthy donors. Donors in which no clear population of CD1d-restricted δ/αβ T cells were observed were given an arbitrary value of 0.01%. Horizontal line indicates the mean.

RESULTS

Identification of CD1d-restricted δ/αβ T cells

We previously identified CD1d-restricted, α-galactosylceramide (α-GalCer)–reactive Vδ1⁺ T cells (Uldrich et al., 2013). Further analysis of human Vδ1⁺ CD1d–α-GalCer tetramer⁺ T cells using a different anti-Vδ1 clone (A13) compared with our previous study (clone TS8.2; Uldrich et al., 2013) revealed that some Vδ1⁺ cells coexpressed a TCR-β chain rather than a TCR-γ chain (Fig. 1 a). Single cell TCR sequencing of individual Vδ1⁺ TCR-β⁺ CD1d–α-GalCer tetramer⁺ T cells confirmed the expression of the Vδ1 gene recombined to Jα gene and Cα constant region (Fig. 1 b).

Downloaded from http://rupress.org/jem/article-pdf/211/13/2599/1749468/jem_20141764.pdf by guest on 08 February 2026

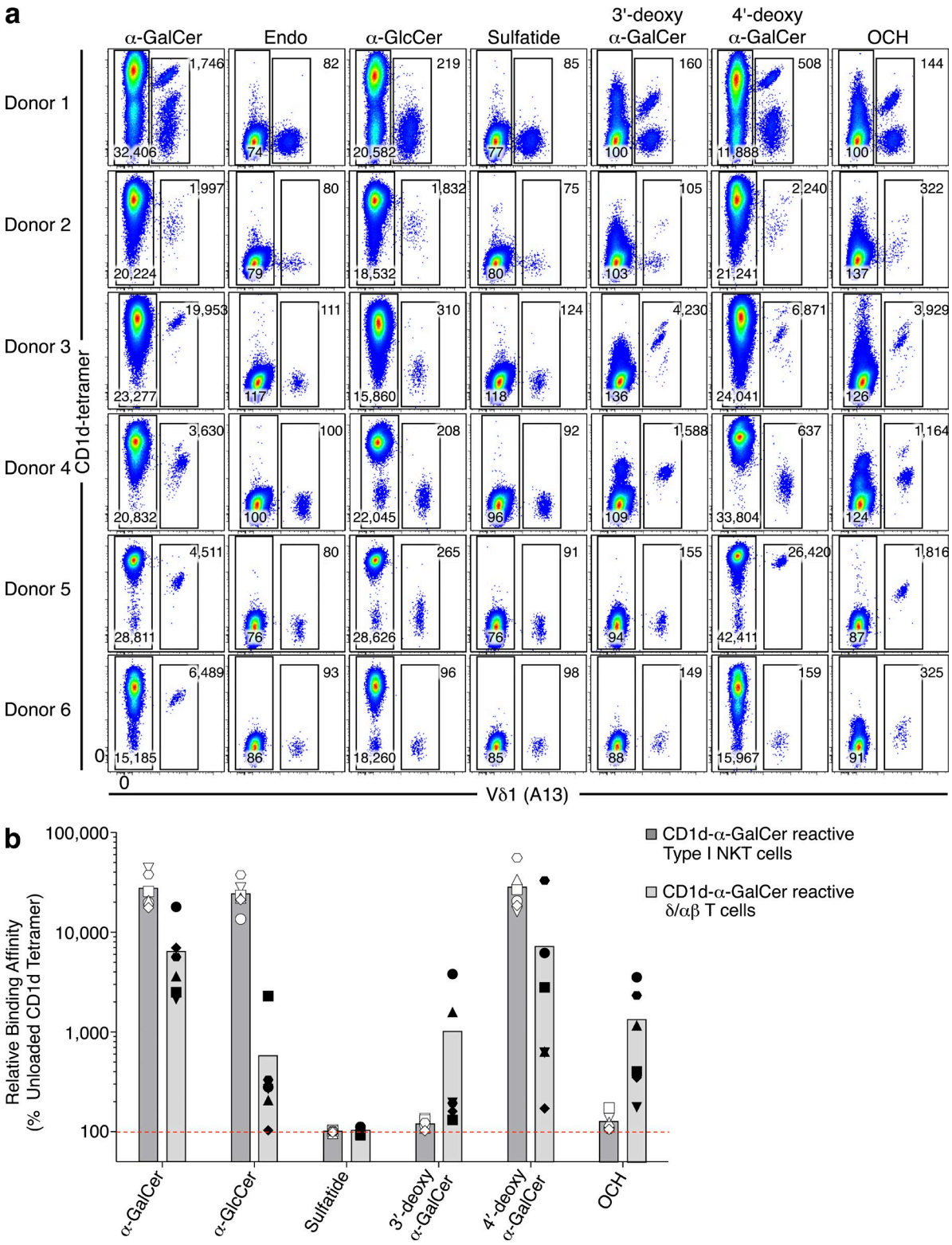

Figure 2. Lipid Ag reactivity of δ/αβTCR⁺ T cells. (a) PBMCs from healthy donors were treated as in Fig. 1 a and analyzed by flow cytometry. Plots show CD1d–α-GalCer tetramer–enriched and in vitro expanded PBMCs, depicting CD1d tetramer versus Vδ1 staining on CD3⁺ γδTCR⁻ cells using a panel of lipid Ag tetramers. Numbers on each plot represent the mean fluorescence intensity within gated regions. (b) The relative binding affinity, based on mean fluorescence intensity, of each lipid Ag is shown for type I NKT cells (CD3⁺ CD1d–α-GalCer⁺ γδTCR⁻ Vδ1⁻, open symbols) and for CD1d-restricted δ/αβTCR⁺ cells (CD3⁺ CD1d–α-GalCer⁺ γδTCR⁻ Vδ1⁺, closed symbols). Data were normalized against endogenous CD1d tetramer (indicated by the dashed red line). Each donor is represented by a different symbol.

Downloaded from http://rupress.org/jem/article-pdf/211/13/2599/1749468/jem_20141764.pdf by guest on 08 February 2026

TCR sequence analysis of these cells from five different donors revealed nine distinct hybrid Vδ1-Jα-Cα-TCR-β chains from within the Vδ1$^+$ CD1d–α-GalCer tetramer$^+$ population (Fig. 1 b). Thus, the Vδ1-specific antibody (clone A13) was capable of recognizing TCRs where the Vδ1 gene is recombined to Jα and Cα genes, whereas the other Vδ1-specific antibody (clone TS8.2) did not bind to these hybrid TCRs (not depicted). Accordingly, we termed CD1d–α-GalCer tetramer$^+$ cells that express δ/αβTCRs as CD1d-restricted δ/αβ T cells.

In contrast to many of the CD1d-restricted Vδ1$^+$ γδ T cells identified in our previous study that were only partially dependent on CD1d-bound lipid Ag (Uldrich et al., 2013), CD1d-restricted δ/αβ T cells showed an absolute requirement for CD1d-Ag, as "unloaded" ("CD1d/Endo") human CD1d tetramers failed to bind these cells (Fig. 1 a). Analysis of in vitro expanded type I NKT cells, CD1d-restricted γδ T cells, and CD1d-restricted δ/αβ T cells revealed that the CD1d-restricted δ/αβ T cells typically expressed low levels of CD161 (not depicted). Despite the ability of Vδ1 to pair with several different TCR-β chains (Fig. 1 b), the TCR-β chain (Vβ11) common to type I NKT cells, was not detected on CD1d-restricted δ/αβ T cells (Fig. 1 a). CD4 and CD8 expression by δ/αβ T cells varied between donors and they were mostly CD4$^+$CD8$^-$ or CD4$^-$CD8$^+$ (Fig. 1 a), and this typically differed from CD4 and CD8 expression on type I NKT cells from within the same donors. Similar to CD1d-restricted γδ T cells (Uldrich et al., 2013), human CD1d-restricted δ/αβ T cells did not stain with mouse CD1d–α-GalCer tetramer, unlike human type I NKT cells which showed strong cross-reactivity to mouse CD1d (not depicted; Brossay et al., 1998). We detected a clear population of CD1d-restricted δ/αβ T cells within the expanded CD1d–α-GalCer–reactive T cell population in 13 out of 30 donors (Fig. 1 c). In most cases, CD1d-restricted δ/αβ T cells represented <1% of total CD1d–α-GalCer–reactive cells, although they were higher in some individuals, including one individual in which they were over 50% of CD1d–α-GalCer–reactive cells (Fig. 1 c). Accordingly, CD1d-restricted δ/αβ T cells represent a novel subset of human CD1d–α-GalCer–restricted T cells, which are distinct from both type I NKT cells and CD1d-restricted γδ T cells.

Ag specificity of δ/αβ CD1d-restricted T cells

To evaluate the Ag specificity of CD1d-restricted δ/αβ T cells, CD1d–α-GalCer tetramer$^+$ cells were isolated and expanded from six different donor PBMC samples and stained with CD1d tetramers loaded with α-GalCer, α-glucosylceramide (α-GlcCer), sulfatide, 3′-deoxy-α-GalCer, 4′-deoxy-α-GalCer, and OCH, known NKT cell ligands (Wun et al., 2011; Rossjohn et al., 2012). Tetramer staining of CD1d-restricted δ/αβ T cells was compared with tetramer staining of type I NKT cells from the same donors (Fig. 2, a and b). CD1d-restricted δ/αβ T cells bound α-GalCer–loaded CD1d tetramer in an Ag-dependent manner as these cells failed to stain with unloaded CD1d tetramer containing endogenous ("endo") Ag (Fig. 2, a and b). Most CD1d-restricted δ/αβ T cells, with the exception of these cells from donor 2, did not bind to CD1d–α-GlcCer tetramer, which is in stark contrast to type I NKT cells from the same donors that stained brightly with this tetramer (Fig. 2, a and b). The CD1d-restricted δ/αβ T cells were also unreactive to sulfatide-loaded CD1d tetramer, whereas reactivity against 3′-deoxy- and 4′-deoxy-α-GalCer was highly variable between individual donors (Fig. 2, a and b). We have previously established that human type I NKT cells are very sensitive to the loss of the 3′-OH group on α-GalCer (Wun et al., 2012). In contrast, we show here that in at least some individuals, human CD1d-restricted δ/αβ T cells (from donors 1, 3, and 4) were clearly stained by the CD1d-3′-deoxy-α-GalCer tetramer, whereas most of the type I NKT cells from those same donors were not (Fig. 2, a and b). Conversely, CD1d-restricted δ/αβ T cells from donors 4 and 6 stained poorly with CD1d-4′-deoxy-α-GalCer tetramers, whereas the type I NKT cells from the same donors were brightly labeled (Fig. 2, a and b). Furthermore, CD1d-restricted δ/αβ T cells from donor 5 showed considerably brighter staining with 4′-deoxy-α-GalCer compared with CD1d–α-GalCer tetramer (Fig. 2, a and b). Reactivity of CD1d-restricted δ/αβ T cells against the OCH Ag showed that δ/αβ T cells from four donors (1, 3, 4, and 5) were capable of binding to this Ag (Fig. 2, a and b), whereas, as expected, most type I NKT cells failed to bind OCH (Matulis et al., 2010; Wun et al., 2011). Collectively, these data highlight that CD1d-restricted δ/αβ T cells are capable of recognizing glycolipids presented by CD1d, and the δ/αβTCR composition imbues these cells with a different pattern of glycolipid Ag specificity that distinguishes them from type I NKT cells from the same donors.

δ/αβ T cells are abundant within human PBMCs

Having determined that some δ/αβ T cells were present within the CD1d–α-GalCer–reactive T cell population, we next examined δ/αβTCRs within the general population of Vδ1$^+$ T cells in humans by analyzing freshly isolated PBMCs. Using the anti-Vδ1 antibody clone A13, we determined that many Vδ1$^+$ T cells coexpress a TCR-β chain, rather than a TCR-γ chain, and are therefore δ/αβ T cells rather than γδ T cells (Fig. 3 a). The ratio of δ/αβ to γδ T cells within the Vδ1$^+$ population varied widely, from <5% to >80% δ/αβ T cells, with a mean of ∼45% (Fig. 3 b). Further investigation of the cell surface phenotype of δ/αβ T cells, in comparison with αβ T cells, revealed that δ/αβ T cells can coexpress CD4 or CD8, although the ratio of CD4 to CD8 was generally different from that observed for αβ T cells, with more CD8$^+$ and less CD4$^+$ δ/αβ T cells than αβ T cells ($P < 0.05$; Wilcoxon paired ranked test). γδ T cells from the same donors were predominantly CD4$^-$CD8$^-$ or CD8$^+$ (Fig. 3 c). TCR-Vβ profiling of these cells indicated that they express a broad range of TCR-β chains, and moreover, the representation of Vβ chains used by δ/αβ T cells did not necessarily parallel that of the αβ T cells from the same donors (Fig. 3 d). This is exemplified by the Vβ8 population, which ranged

Downloaded from http://rupress.org/jem/article-pdf/211/13/2599/1749468/jem_20141764.pdf by guest on 08 February 2026

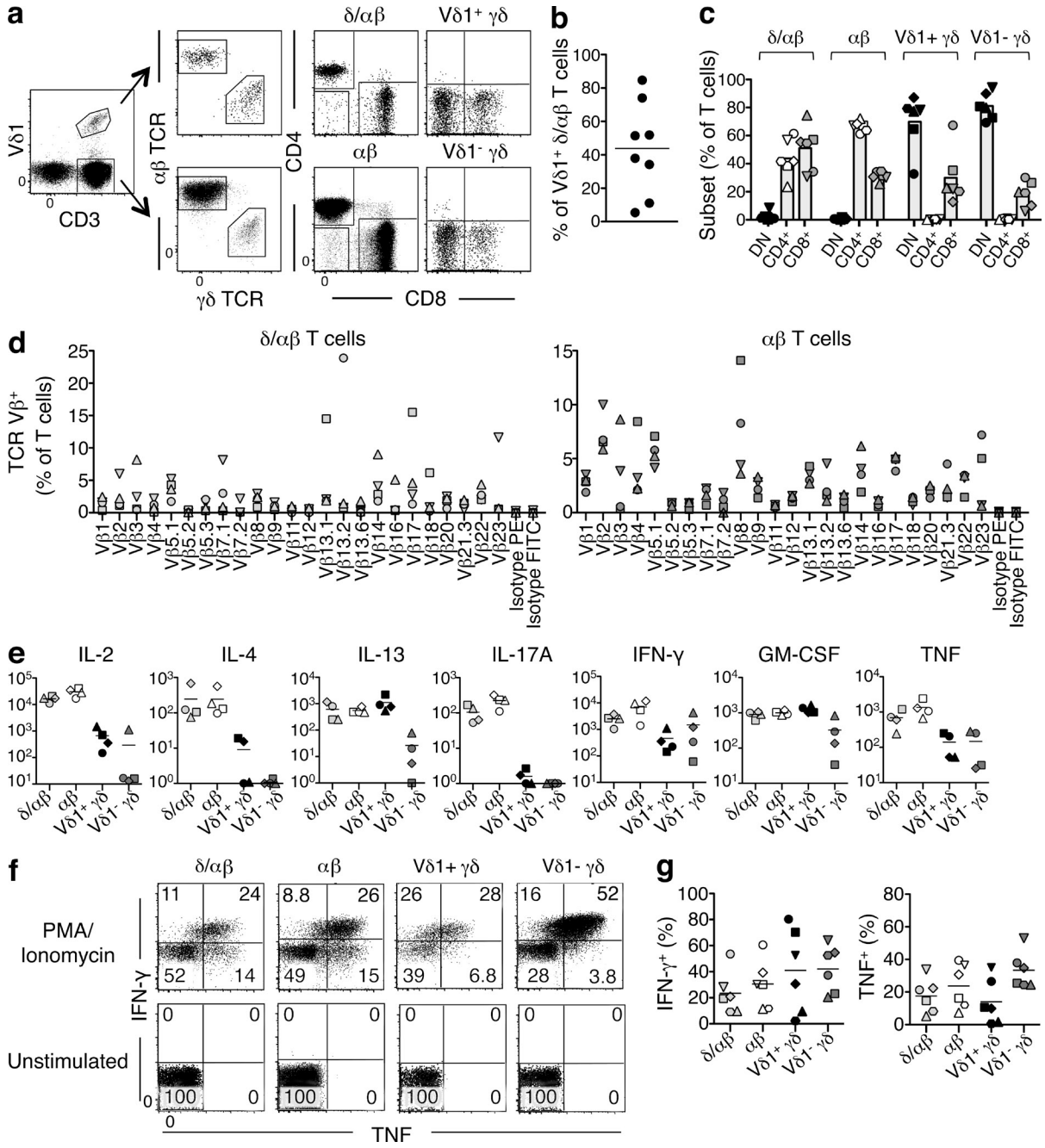

Figure 3. TCR-Vδ1⁺ cells consist of γδTCR⁺ and δ/αβTCR⁺ subsets. (a) CD14⁻ CD19⁻ lymphocytes from a representative healthy blood donor, were analyzed by flow cytometry. Plots show CD3⁺ Vδ1⁺ and CD3⁺ Vδ1⁻ PBMC subsets, gated as indicated (left plot), and then subsets labeled with anti-αβTCR (identifying δ/αβ T cells and αβ T cells) versus anti-γδTCR (identifying γδ T cells) are shown (second plots). Expression of CD4 and CD8 on these subsets is also shown (right-hand plots). (b) The percentage of Vδ1⁺ cells that were αβTCR⁺ (i.e., δ/αβ T cells) was calculated for eight donors using the gating strategy shown in a. (c) The percentage of CD4⁻ CD8⁻ (double negative [DN]), CD4⁺ CD8⁻ (CD4⁺), and CD4⁻ CD8⁺ (CD8⁺) cells within Vδ1⁺ αβTCR⁺ (δ/αβ), Vδ1⁻ αβTCR⁺ (αβ), Vδ1⁺ γδTCR⁺ (Vδ1⁺ γδ), and Vδ1⁻ γδTCR⁺ (Vδ1⁻ γδ) is shown, with each symbol representing a separate donor ($n = 6$) and bar graphs depicting the mean value. (d) Healthy human PBMCs were stained with a panel of anti–TCR-Vβ–specific antibodies. Plots show the percentage of Vδ1⁺ αβTCR⁺ (δ/αβ, left) and Vδ1⁻ αβTCR⁺ (αβ, right) T cells that bound to each Vβ antibody. Graphs depict $n = 4$ donors with each symbol representing a different donor. (e) δ/αβ T cells, αβ T cells, Vδ1⁺ γδ T cells, and Vδ1⁻ γδ T cells (as defined in c) were purified by FACS and stimulated with anti-CD3/CD28 beads for 72 h. Cytokines in culture supernatants were measured by cytometric bead array. Each data point represents the mean of $n = 2$–4 replicates from one donor, with $n = 4$ donors and each symbol shape representing a different donor. (f) δ/αβ, αβ, Vδ1⁺ γδ, and Vδ1⁻ γδ T cells from a representative donor (as defined in c) were stimulated for 4 h with PMA/ionomycin (top plots) or unstimulated (bottom plots), and IFN-γ and TNF were measured by intracellular cytokine staining. (g) Percentage of IFN-γ– and TNF-producing cells stimulated as in e, with each symbol representing a separate donor ($n = 6$). Symbols indicating specific donors within panels do not correlate with the same donors between different panels. (b, e, and g) Horizontal lines indicate the mean.

Downloaded from http://rupress.org/jem/article-pdf/211/13/2599/1749468/jem_20141764.pdf by guest on 08 February 2026

from 3 to 15% of αβ T cells in four donors, whereas δ/αβ T cells from the same four donors were <3% Vβ8$^+$. Thus, these data highlight that Vδ1$^+$ δ/αβ T cells are present in similar frequency to Vδ1$^+$ γδ T cells in human peripheral blood. Moreover, aside from their unusual TCR, δ/αβ T cells are also distinct from both αβ and γδ T cells with regard to their CD4 or CD8 coexpression profiles and TCR-β repertoire.

δ/αβTCRs transmit activation signals

Using flow cytometric sorting, we purified δ/αβ, αβ, and γδ T cells from several human donors and stimulated them in vitro for 3 d in the presence of anti-CD3– and CD28-coated beads to measure their relative ability to produce cytokines in response to TCR cross-linking. These results (Fig. 3 e) demonstrated that δ/αβ T cells are responsive to TCR cross-linking, resulting in abundant cytokine production, including IL-2, IL-4, IL-13, IL-17, IFN-γ, GM-CSF, and TNF, at levels comparable with that of αβ T cells and clearly distinct from that observed for both Vδ1$^+$ and Vδ1$^-$ γδ T cells from matched donors. The response from the γδ T cells was generally lower than that of the δ/αβ T cells for IL-2, IFN-γ, and TNF, whereas the Vδ1$^+$ γδ T cells produced comparable GM-CSF and IL-13 to the δ/αβ T cells after anti-CD3/CD28 stimulation (Fig. 3 e). To examine the cytokine-producing potential of these different cell types further, we compared all four subsets after a brief (4 h) stimulation with PMA and ionomycin and measured IFN-γ and TNF by intracellular cytokine staining (Fig. 3, f and g). These data indicated that both Vδ1$^+$ and Vδ1$^-$ γδ T cells can produce abundant IFN-γ and TNF and thus were functionally similar using this method of stimulation.

We next wanted to determine whether direct ligation of the δ/αβTCR with defined Ag could result in cellular activation. To achieve this, we stably transduced a CD1d-restricted δ/αβTCR (clone 9B4) and an irrelevant pHLA-reactive TCR into the αβTCR-deficient Jurkat-76 cell line and cultured these cells in the presence of α-GalCer or α-GlcCer. As these cell lines express CD1d (not depicted), no Ag-presenting cells were added. CD69 up-regulation was used as an indicator of Ag-mediated cellular activation (Fig. 4, a and b). Type I NKT TCR (NKT15)–transduced SKW3 cells, which also express CD1d, were included as a positive control in this assay. The control HLA-restricted TCR-transduced cells did not respond to either glycolipid Ag. These experiments demonstrated that the δ/αβTCR was capable of recognizing α-GalCer Ag presented by CD1d and, furthermore, that this recognition event could transmit cellular activation signals (Fig. 4 a). Also, although NKT15 TCR-transduced cells were capable of recognizing α-GalCer and α-GlcCer equally, the δ/αβTCR-transduced cells were only capable of responding to α-GalCer (Fig. 4 b), consistent with our CD1d tetramer staining of CD1d-restricted δ/αβ T cells from in vitro expanded PBMCs (Fig. 2). Furthermore, the δ/αβTCR-transduced cells responded to three different analogues of α-GalCer with different acyl chains, including C24:1 (Fig. 4 a), C20:2 (Fig. 4 b), and C26 analogues (not depicted). Collectively,

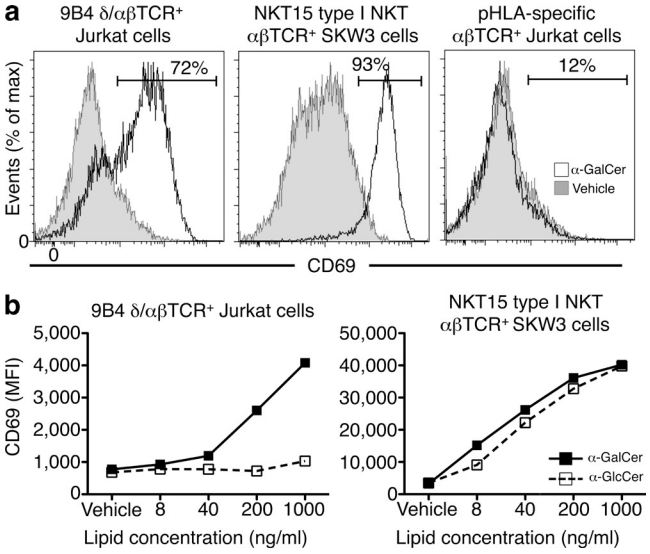

Figure 4. α-GalCer activates a 9B4 δ/αβTCR$^+$ cell line in vitro. (a) CD69 expression was measured on cell lines, including 9B4 δ/αβTCR-transduced Jurkat cells, NKT15 type I NKT TCR–transduced SKW3 cells, or control pHLA-specific αβTCR-transduced Jurkat cells, after overnight in vitro culture with 1 μg/ml α-GalCer (C24:1) or vehicle alone. (b) CD69 expression on the cell lines (as defined in a) after overnight in vitro culture with graded concentrations of α-GalCer (C20:2 analogue) or α-GlcCer (C20:2 analogue). MFI, mean fluorescence intensity. Data in a and b represent one of two similar experiments in which the other experiments used α-GalCer C26 with similar results to α-GalCer C24:1 in a and α-GalCer C20:2 in b.

these data indicate that δ/αβTCRs are capable of transmitting activating signals in response to specific glycolipid Ags, resulting in cellular activation and diverse cytokine production.

Specificity of 9B4 δ/αβTCR to CD1d-Ag

To study the molecular basis for the binding of a δ/αβTCR to CD1d-Ag, we first determined the specificity of an isolated δ/αβTCR (9B4) for CD1d tetramer–glycolipid, using the same panel of glycolipid Ags as shown in Fig. 2. The pattern was clearly distinct from that of cells transduced with type I NKT TCR (clone NKT15), and cells transduced with an irrelevant pHLA-specific TCR showed no staining with any of the CD1d-Ag tetramers tested. Namely, 9B4 δ/αβTCR-transduced Jurkat cells recapitulated the pattern of reactivity observed for the δ/αβ T cells from donor 1 (Fig. 2), demonstrating strong staining with CD1d tetramers loaded with α-GalCer and 4′-deoxy-α-GalCer, moderate staining with 3′-deoxy-α-GalCer and OCH, and very little reactivity with α-GlcCer and sulfatide-loaded CD1d tetramer (Fig. 5 a).

We next generated a soluble version of this TCR using previously described methods (Kjer-Nielsen et al., 2006), and the soluble 9B4 δ/αβTCR exhibited a molecular mass of 48 kD and reacted with an anti-Vδ1 mAb and an anti-TCR Cα mAb, thereby indicating that the δ/αβTCR had refolded properly (not depicted). Surface plasmon resonance (SPR) was used to investigate the affinity of the interaction between

Downloaded from http://rupress.org/jem/article-pdf/211/13/2599/1749468/jem_20141764.pdf by guest on 08 February 2026

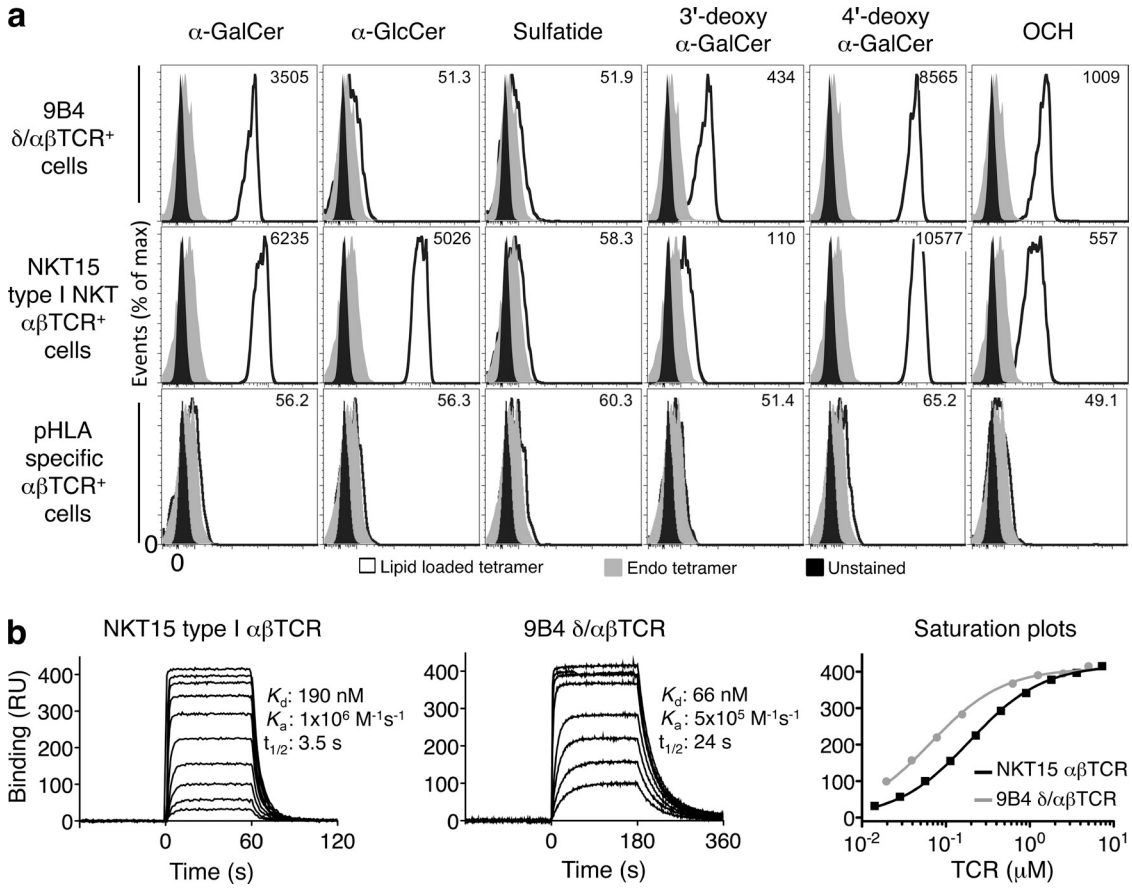

Figure 5. 9B4 δ/αβTCR reacts with CD1d–α-GalCer. (a) Jurkat cell lines expressing the 9B4 δ/αβTCR, NKT15 type I NKT αβTCR, or a control pHLA-specific αβTCR were stained with CD1d tetramers loaded with different lipid Ags (open histograms), compared with endogenous CD1d tetramer staining (gray histograms) or unstained cells (black histograms), and analyzed by flow cytometry. Numbers on histograms depict the mean fluorescence intensity of each lipid-loaded tetramer. (b) Binding affinity of soluble type I NKT TCR (NKT15, left sensorgrams, 7.3 µM to 0.014 µM) and δ/αβTCR (9B4, middle sensorgrams, 5 µM to 0.02 µM) was assessed using SPR. Interactions were measured with CD1d–α-GalCer. Saturation plots (right) depict binding at equilibrium of 9B4 and NKT15 TCR. RU, response units; K_d, dissociation constant; K_a, association rate; $t_{1/2}$, half-life. Data are from one of two independent experiments.

the 9B4 δ/αβTCR and CD1d loaded with C26:0 α-GalCer (Fig. 5 b). The human NKT15 type I Vα24$^+$ αβTCR (Kjer-Nielsen et al., 2006) was included as a positive control (Fig. 5 b). No notable autoreactivity to CD1d-endogenous was observed for the 9B4 δ/αβTCR, in stark contrast to the autoreactivity previously observed for the CD1d-restricted 9C2 γδTCR (Uldrich et al., 2013). The 9B4 δ/αβTCR bound to CD1d–α-GalCer with very high affinity (K_d = 66 nM), even compared with the type I NKT15 αβTCR (K_d = 190 nM; Fig. 5 b), and markedly higher than the 9C2 Vδ1$^+$ γδTCR (K_d of 15 µM; Uldrich et al., 2013). This higher affinity of the 9B4 δ/αβTCR is partly caused by a slower dissociation rate (half-life of 24 s compared with 3.5 s for the NKT15 αβTCR). Thus, the 9B4 δ/αβTCR binds strongly to CD1d–α-GalCer and is highly sensitive to the type of CD1d-restricted lipid Ags presented.

The δ/αβTCR–CD1d-Ag complex

To understand how the 9B4 δ/αβTCR recognized CD1d–α-GalCer, we determined the crystal structure of the ternary complex (Fig. 6 a and Table S1) as well as the nonliganded 9B4 TCR (Table S1). The 9B4 TCR docked orthogonally (73°) above the A′ pocket of CD1d, relative to the CD1d cleft, burying ∼1,050 Å^2, and interacted with residues ranging from 58 to 79 of the α1 helix and from 153 to 171 of the α2 helix of CD1d (Fig. 6, a and b). This mode of recognition differed markedly from type I NKT TCR–CD1d–α-GalCer recognition, whereupon the Vα24-Vβ11 TCR sat parallel over the F′ pocket of CD1d (Fig. 6, a and b; Borg et al., 2007). Accordingly, the interatomic contacts and roles of the individual CDR loops at the type I NKT TCR–CD1d–α-GalCer interface were markedly different to those at the 9B4 TCR–CD1d–α-GalCer interface (Fig. 6 c). Indeed, the δ/αβTCR–CD1d–α-GalCer complex was more similar to the 9C2 γδTCR–CD1d–α-GalCer complex (Fig. 6, a–c), which sat orthogonally (83°) over the A′ pocket (buried surface area [BSA] of ∼950 Å^2), although the 9B4 TCR variable regions were shifted more toward to the center of the CD1d cleft (shift of 7 Å for the TCR-β chain and 3 Å for the TCR-Vδ/α chain, relative to the 9C2 TCR-γ and -δ chains,

Downloaded from http://rupress.org/jem/article-pdf/211/13/2599/1749468/jem_20141764.pdf by guest on 08 February 2026

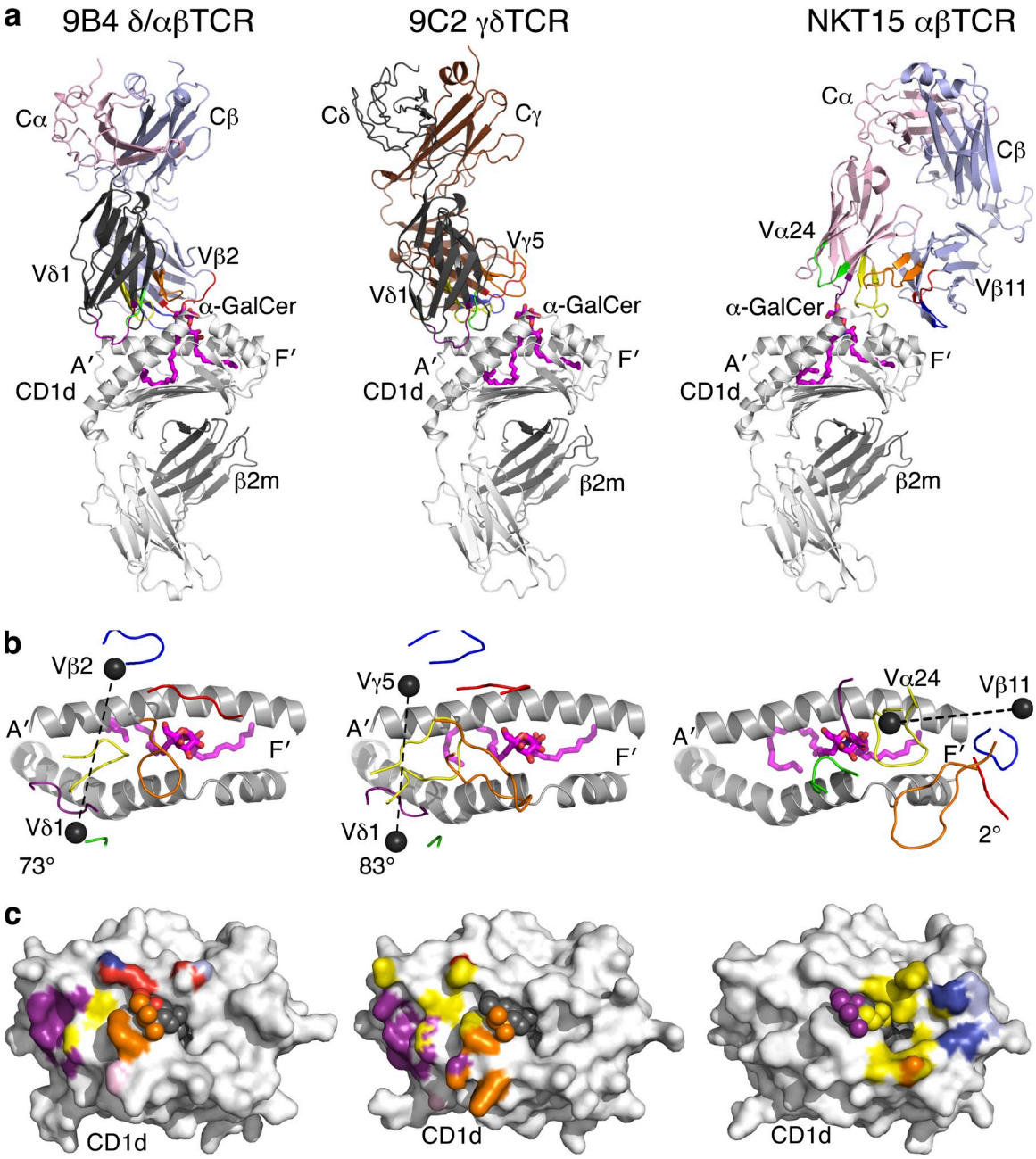

Figure 6. Structure of CD1d–α-GalCer complexed with the 9B4 δ/αβTCR. (a) Overview of the 9B4 δ/αβTCR bound to CD1d–α-GalCer (left) compared with the 9C2 γδTCR bound to CD1d–α-GalCer (middle, PDB code 4LHU [Uldrich et al., 2013]) and the NKT15 type 1 NKT TCR bound to CD1d–α-GalCer (right, PDB code 2PO6 [Borg et al., 2007]). TCR-δ, black; TCR-β, light blue; TCR-α, pink; TCR-γ, brown; CD1d, white; β2-microglobulin, gray; α-GalCer, pink sticks; CDR1α and CDR1δ, purple; CDR2α and CDR2δ, green; CDR3α and CDR3δ, yellow; CDR1β and CDR1γ, red; CDR2β and CDR2γ, blue; and CDR3β and CDR3γ, orange. (b) CD1d molecules of 9B4 (left), 9C2 (middle), and NKT15 (right) using color scheme as per a. Black spheres represent the center of mass of the indicated variable domains, with the docking angles indicated by the dotted lines. (c) Structural footprint of the 9B4 (left), 9C2 (middle), and NKT15 (right) TCRs on the CD1d–α-GalCer complex. CDR loops are colored as per a and b, and the α-GalCer lipid Ags are represented as spheres.

respectively), thereby bringing the δ/αβTCR closer to the α-GalCer headgroup.

The δ/αβTCR-mediated recognition of CD1d was dominated by the Vδ1 chain (66% of the total BSA), relative to the Vβ2 chain (33% of the total BSA; Table S2). For the TCR-β chain, both the CDR1β and CDR3β made contributions to the interface (13% and 11% of the total BSA, respectively; Figs. 6 c and 7 a). Namely, the aliphatic moiety of Arg79 of CD1d was pincered by Gln29β from the CDR1β loop and the framework residue Leu77β (Fig. 7 a). In addition, Arg79

Downloaded from http://rupress.org/jem/article-pdf/211/13/2599/1749468/jem_20141764.pdf by guest on 08 February 2026

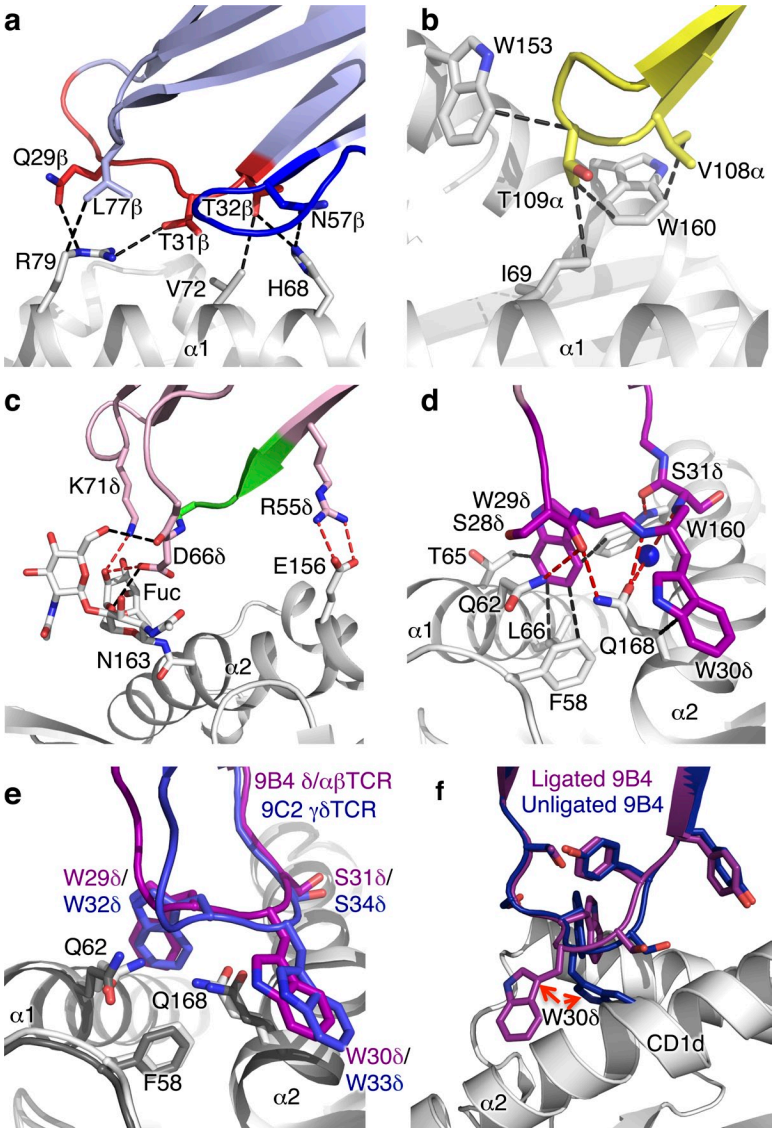

Figure 7. Interactions at the interface of the 9B4 δ/αβTCR and CD1d. (a) Interactions between the TCR-β chain (in light blue) and CD1d (in white), showing the 9B4 TCR CDR1β loop (in red) and CDR2β loop (in blue). (b) Interactions between the 9B4 TCR CDR3δ/α loop (in yellow) and CD1d (in white). (c) Interactions between the 9B4 TCR-α chain (in light pink) and CD1d (in white), showing the 9B4 TCR CDR2δ loop (in green). Fuc, fucose. (d) Interactions between the 9B4 TCR CDR1δ loop (in purple sticks) and CD1d (in white). (e) Comparison of the 9B4 TCR CDR1δ loop (in purple) and the 9C2 γδTCR CDR1δ loop (in blue, PDB code 4LHU [Uldrich et al., 2013]) after superposition of CD1d from the 9C2 ternary structure (in black) onto CD1d from the 9B4 ternary structure (in white). (f) Comparison of the 9B4 δ/αβTCR CDR1δ loop, derived from the unligated state (blue sticks) and the ligated state (purple sticks), along with CD1d (white cartoon). The red dashed lines indicate hydrogen bonds, and the black dashed lines represent van der Waals forces.

contacted Thr31β, which, together with the adjacent Thr32β, packed against Val72 from CD1d, with Thr32β and Asn57β also interacting with His68 of CD1d (Fig. 7 a). The CDR3δ/α loop (13% of the total BSA) extended toward the α2 helix of CD1d, with its main chain packed against α-GalCer (discussed below) and contacted residues from the α1 and α2 helices (Fig. 7 b). Namely, Trp160 of CD1d was positioned between Val108α and Thr109α, the latter of which also contacted Ile69 and Trp153 of CD1d (Fig. 7 b). Trp153 is a position that differs in mouse CD1d (Gly155; Godfrey et al., 2005), thereby providing a basis of why the δ/αβTCR does not cross-react onto mouse CD1d–α-GalCer (not depicted).

The Vδ1-mediated contacts with CD1d are dominated by the CDR1δ loop (38% of the total BSA), with further contributions from the framework region (15% BSA; Table S2). Although the CDR2δ loop did not interact with CD1d, the flanking framework regions did (Fig. 7 c). Here, Arg55δ extended down toward the α2 helix to form a salt bridge with Glu156, whereas Asp66δ and Lys71δ mediated contacts with the glycosylation site attached to Asn163 of CD1d (Fig. 7 c). These framework-mediated interactions with CD1d were analogous to those observed in the 9C2 γδTCR–CD1d-Ag complex (Uldrich et al., 2013).

The CDR1δ loop sat over the distal end of the A′ pocket of CD1d and exclusively contacted CD1d (Fig. 7 d). The interactions were dominated by two Trp residues (Trp29 and Trp30) that were flanked by Ser residues (Ser28δ and Ser31δ) whose side chains formed vdw interactions with CD1d, while their main chains hydrogen bonded with CD1d residues (Gln62, Gln168, and Trp160; Fig. 7 d). Trp29δ was wedged between the α1 and α2 helices of CD1d, packed against the aliphatic side chains of Gln62, Thr65, and Leu66 and the aromatic ring of Trp160 (Fig. 7 d). Trp30δ was positioned at the periphery of CD1d, stacked principally against Gln168 (Fig. 7 d).

Downloaded from http://rupress.org/jem/article-pdf/211/13/2599/1749468/jem_20141764.pdf by guest on 08 February 2026

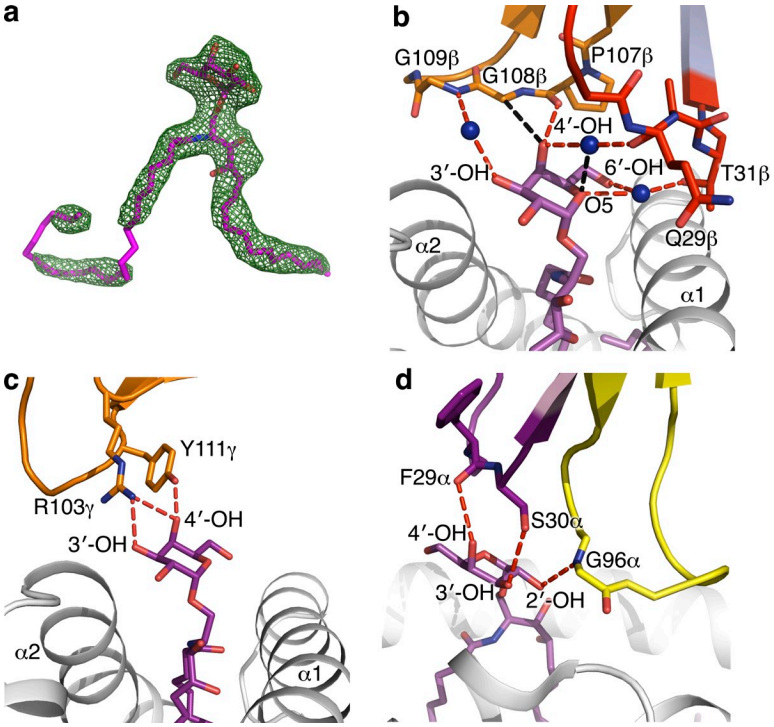

Figure 8. Interactions with α-GalCer. (a) Shows the *Fo-Fc* omit electron density map of the α-GalCer Ag in green, contoured at 3 σ. (b) Interactions between the 9B4 TCR and α-GalCer, showing the CDR1β (in red sticks), CDR3β (in orange sticks), CD1d (white), and α-GalCer (dark pink sticks). (c) Interactions between the 9C2 TCR CDR3γ (in orange) and α-GalCer (dark pink sticks; PDB code 4LHU [Uldrich et al., 2013]). (d) Interactions between the NKT15 NKT cell αβTCR CDR1α (in purple) and CDR3α (in yellow) and α-GalCer (dark pink sticks; PDB code 2PO6 [Pellicci et al., 2009]). Water molecules are shown as blue spheres, the red dashed lines represent hydrogen bonds, and the black dashed lines represent van der Waals interactions between the residues in all schematics.

These CDR1δ loop–mediated contacts by the δ/αβTCR were very similar to those observed in the 9C2 γδTCR–CD1d-Ag structure (Fig. 7 e). Thus, the germline-encoded regions of the Vδ1 domain of the δ/αβTCR adopted a very similar mode of CD1d-Ag recognition as the γδTCR. This showed that Vδ1 is not only capable of binding CD1d when rearranged with a Dδ-Jδ–encoded CDR3δ motif (in the context of a γδTCR), but also when rearranged with a permissive Jα segment in the context of a δ/αβTCR.

The structure of 9B4 TCR in the unligated state enabled us to assess the extent of plasticity of the CDR loops upon CD1d–α-GalCer engagement. Upon ligation, the 9B4 TCR variable regions did not significantly change conformation (root-mean-square deviation [rmsd] 0.5 Å for both Vδ1 and Vβ2); however, surprisingly, the positioning of the constant regions was significantly altered by approximately a 17° shift in the elbow angle between the V and C domains in a direction toward the F′ pocket of CD1d (not depicted). In contrast, there was minimal change in the conformation of the CDR loops upon ligation (rmsd ranging from 0.3 to 1 Å), with the biggest alteration observed for Trp30 of the CDR1δ loop, which flipped upon ligation to avoid clashing with the α2 helix of CD1d (Fig. 7 f). Thus, analogous to αβTCR and γδTCR recognition of CD1d–α-GalCer, a rigid "lock-and-key" mechanism underpinned δ/αβTCR ligation (Borg et al., 2007; Pellicci et al., 2009; Uldrich et al., 2013).

Lipid Ag recognition

The electron density at the interface and for the α-GalCer Ag in the 9B4 ternary complex was unambiguous (Fig. 8 a), thereby permitting a comparison of how three TCRs arising from distinct lineages, the αβTCR, the γδTCR, and the δ/αβTCR, interacted with the same Ag-presenting molecule bound to the same ligand. Although the 9B4 TCR-Vδ1 chain dominated the interaction with CD1d, α-GalCer recognition was mediated entirely by the TCR-β chain, specifically being sequestered by the CDR1β and CDR3β loops via a polar interaction network. This recognition is notably dominated by water-mediated contacts and interactions that involved the main chain of the δ/αβTCR (Fig. 8 b). Namely, all of the hydroxyl moieties of the α-GalCer headgroup, with the exception of the 2′-OH moiety, were involved in hydrogen bonding with the TCR-β chain of the δ/αβTCR. Specifically, Pro107β hydrogen bonded to the 4′-OH, whereas three water-mediated hydrogen bonds were formed between Gln29β, Thr31β, and Gly109β and the 4′-OH, 6′-OH, and 3′-OH moieties of α-GalCer, respectively (Fig. 8 b).

The structural basis for α-GalCer recognition by the δ/αβTCR was markedly distinct to that mediated via the 9C2 γδTCR and the NKT15 αβTCR (Fig. 8, b–d; Borg et al., 2007; Pellicci et al., 2009; Uldrich et al., 2013). Within the γδTCR–CD1d–α-GalCer complex, the CDR3γ loop exclusively contacted the α-GalCer headgroup, with Arg103γ and Tyr111γ hydrogen bonded to the 3′-OH and 4′-OH moieties (Fig. 8 c; Uldrich et al., 2013). In the NKT15 complex, the interactions with α-GalCer were exclusively mediated via the invariant TCR-α chain, where the α-GalCer headgroup sat underneath the CDR1α loop and abutted the CDR3α loop (Fig. 8 d; Borg et al., 2007; Pellicci et al., 2009). Here, the galactose 2′-OH, 3′-OH, and 4′-OH moieties were involved in

Downloaded from http://rupress.org/jem/article-pdf/211/13/2599/1749468/jem_20141764.pdf by guest on 08 February 2026

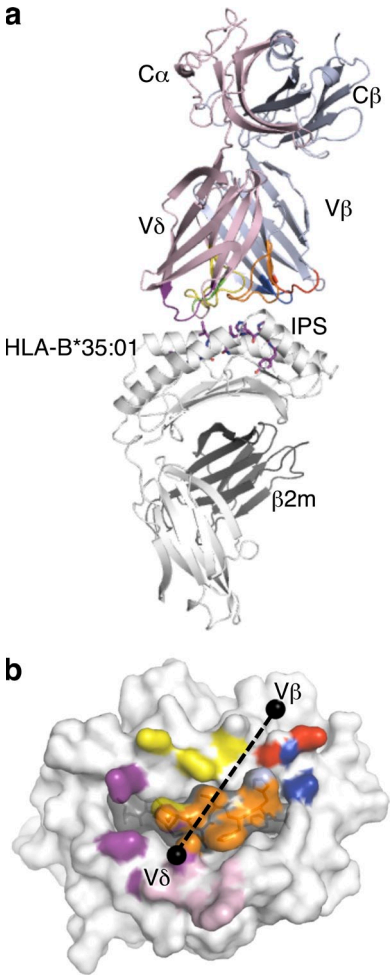

Figure 9. Clone 12 TCR–HLA-B*35:01–IPS structure. (a) Overview of the clone 12 TCR (δ/α chain in pale pink, β chain in pale blue) in complex with the IPS peptide (purple sticks) bound to the HLA-B*35:01 molecule (white cartoon) and β-2-microglobulin (β2m, black cartoon). The clone 12 TCR CDR loops are colored in purple, green, and yellow for the CDR1/2/3δ/α and red, blue, and orange for the CDR1/2/3β. (b) Atomic footprint of the clone 12 TCR, colored by CDR loops according to panel a, on the surface of the IPS peptide (gray surface) bound to the HLA-B*35:01 molecule (white surface). The black spheres represent the mass center of the Vδ/α and Vβ domains.

polar-mediated contacts with the αβTCR. Accordingly, the αβTCR, γδTCR, and δ/αβTCRs contact the same lipid Ag via markedly distinct binding mechanisms.

Molecular basis of δ/αβTCR recognition of pHLA-I

We determined that there are many other δ/αβTCRs in healthy humans (Fig. 3), although the specificity of these cells is unclear. Nevertheless, previously, we had described a panel of T cell clones that were restricted to HLA-B*35:01 presenting a 9-mer epitope (IPSINVHHY [IPS]) originating from the pp65 Ag of CMV (Amir et al., 2011). We noted that one of these T cell clones, clone 12, expressed the same Vδ1-Jα52-Cα rearrangement as the 9B4 TCR, albeit with a different CDR3δ/α sequence and TCR-β chain gene usage (Vβ5.1-Jβ2.1). Thus, we formally investigated how this $Vδ1^+$ δ/αβTCR mediated an MHC-restricted response.

Using SPR, we established that the clone 12 δ/αβTCR exhibited a 15 μM affinity for the HLA-B*35:01–IPS complex (not depicted), which fell within the normal affinity range observed for αβTCR–MHC-I interactions (Gras et al., 2012). Next, we solved the structure of the clone 12 δ/αβTCR in complex with HLA-B*35:01–IPS Ag at 3.0 Å resolution (Fig. 9 and Table S1). The clone 12 TCR docked 56° across the HLA-B*35:01–IPS cleft (Fig. 9 a), within the range of standard αβTCR–pHLA-I complexes (Gras et al., 2012). In addition, the clone 12 TCR ternary complex possessed features typically associated with αβTCR–pHLA-I complexes (Gras et al., 2012). For example, the BSA of the TCR interface was 1,014 $Å^2$ (total BSA of the TCR/pHLA interface = 2,040 $Å^2$, within the range of αβTCR–pMHC-I interactions). The clone 12 δ/αβTCR predominantly used its TCR-δ chain (65% BSA) to engage the pHLA complex, where the interaction was dominated by the CDR1δ (27%), CDR3δ/α (20%), and Vδ1 framework (18% BSA) residues, whereas the CDR3β loop was the principal contributor (19% BSA) from the β chain (Fig. 9 b). Although the CDR3β loop mainly contacted the peptide Ag (discussed below), Tyr112β H bonded to Gln155, an MHC residue which is frequently contacted by αβTCRs (Burrows et al., 2010). The other contacts mediated via the β chain included a salt bridge (Arg30β to Glu76) and a hydrogen bond with Asn80 and two residues from the CDR2β loop mediating contacts. Thus the germline-encoded TCR-β chain–MHC contacts were very limited (Table S3 and not depicted).

The long CDR3δ/α loop (17 residues) formed an extended hairpin structure that sat above the HLA α1 helix (residues 65–72), while pointing away from the peptide (Fig. 10 a). Here, two residues from the N-region and two residues from the Jα gene segment were involved in hydrophobic interactions with HLA-B*35:01 (Table S3). Additionally, Thr115δ hydrogen bonded to Thr69 of the α1 helix (Fig. 10 a and Table S3). Interestingly, the clone 12 TCR framework residue Arg55δ interacted with the HLA-B*35:01 molecule in a similar fashion to that observed for the 9B4 interaction with the CD1d molecule (Fig. 8 c), whereby the Arg55δ points toward the α2 helix and hydrogen bonded to Ala150 (Fig. 10 b). In addition, Glu67δ formed a salt bridge with Arg151, and Asp66δ made hydrophobic interactions with Glu154, Gln155, and Ala158 (Fig. 10 b).

The CDR1δ loop, with its two large Trp residues (Trp29δ and Trp30δ), contacted the N-terminal side of the Ag-binding cleft of the HLA-I molecule on both helices (Fig. 10 c). Trp29δ packed against Arg62, whereas Trp30δ extended toward the α2 helix, stacking between the short aliphatic chains of Ala158 and Leu163. Furthermore, another aromatic residue from the CDR1δ loop, Tyr33δ, packed against Gln155. Accordingly, the CDR1δ loop played an extensive role in enabling this HLA-I–restricted response. Nevertheless, the placement of the CDR1δ loop atop the HLA-I and CD1d differed

Downloaded from http://rupress.org/jem/article-pdf/211/13/2599/1749468/jem_20141764.pdf by guest on 08 February 2026

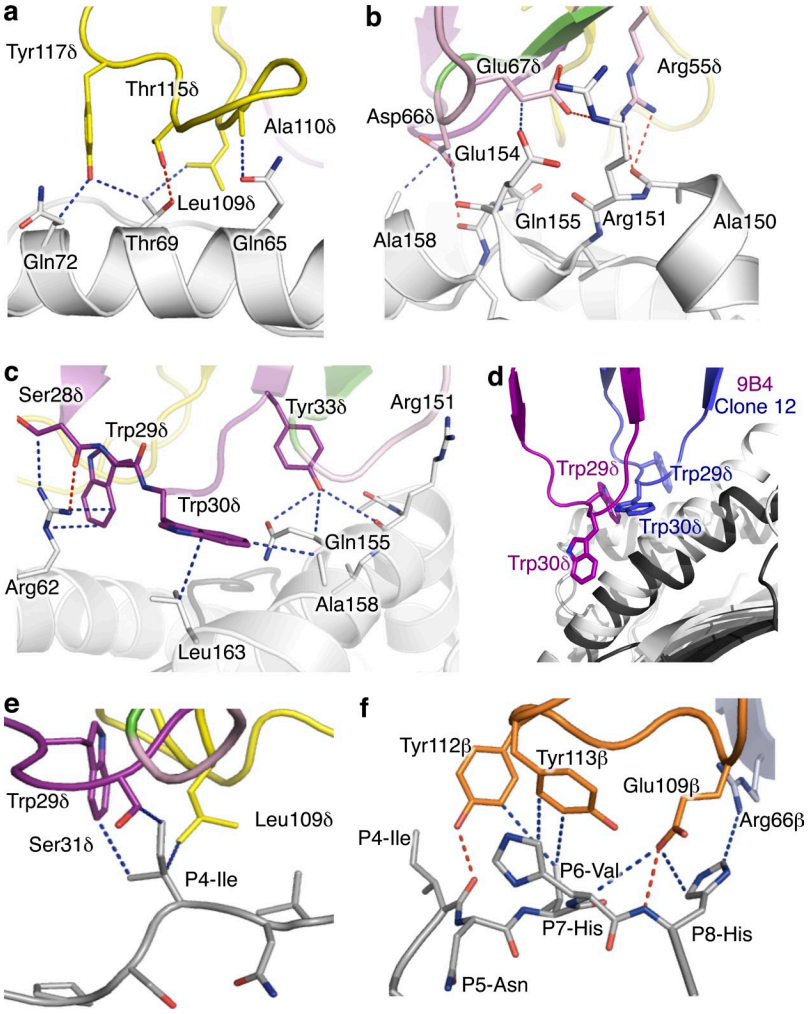

Figure 10. Clone 12 TCR–HLA-B*35:01–IPS interactions. (a–c) The interactions between the HLA-B*35:01 (white cartoon) and the clone 12 TCR CDR3δ/α loop (a), FWδ (b), and CDR1δ loop (c). The CDR loops are colored according to Fig. 9 a. (d) Comparison of the 9B4 TCR CDR1δ loop (in purple) and the clone 12 δ/αβTCR CDR1δ loop (in blue) after superposition of HLA-B*35:01 from the clone 12 ternary structure (in black) onto CD1d from the 9B4 ternary structure (in white). (e and f) The interactions between the clone 12 TCR and the IPS peptide (gray sticks) are represented in e for the Vδ/α chain and f for the Vβ chain. The blue dashed lines represent van der Waals interactions, and the red dashed lines represent hydrogen bonds.

markedly (Fig. 10 d), indicating the versatility of the same germline-encoded region to interact with diverse Ag presentation platforms.

Peptide Ag recognition

Although the TCR-δ chain of clone 12 TCR dominated the interaction with the HLA-I molecule, it made very limited contacts with the IPS peptide. Specifically, the contacts from the δ chain were focused solely onto P4-Ile, which formed hydrophobic contacts with CDR1δ and CDR3δ/α (Fig. 10 e). Notably, however, these Vδ1-driven contacts appeared to play a key role in interacting with P4-Ile, as mutation of the P4-Ile to an Ala dramatically decreased the binding affinity of the δ/αβTCR (K_d > 200 μM; not depicted). The majority of contacts to the IPS epitope were made by the Vβ chain, principally a framework residue (Arg66β) and the CDR3β loop (Fig. 10 f). Arg66β contacted the P8-His, and interestingly, Arg66β is found in the Vβ5, Vβ1, and Vβ6.8 genes only. The structure of Vβ1$^+$ TCR also showed how this framework TCR-β chain residue directly contacted the Epstein-Barr virus–derived epitope (Gras et al., 2010). The CDR3β loop formed most of the interactions with the IPS peptide, contacting the P4-Ile, P6-Val, P7-His, and P8-His residues, and many of these peptide residues were important for the interaction (Fig. 10 f and Table S3). Here, the Tyr112β inserted its aromatic ring between the main chain of the P4-Ile and P6-Val, whereas Tyr113β sat atop the P7-His and contacted the P6-Val (Fig. 10 f). Furthermore, Glu109β contacted P7-His and hydrogen bonded to the main chain of P8-His (Fig. 10 f). Thus, the TCR-β chain plays a major role in mediating contacts with the peptide, with a key contribution from the CDR1δ loop. In summary, we have demonstrated that T cells expressing δ/αβTCRs can recognize both CD1d–glycolipid Ags as well as MHC–peptide Ags and have provided the molecular bases for how these interactions occur.

DISCUSSION

Since the discovery of the TCR genes in the 1980s (Hedrick et al., 1984), considerable insight into αβ T cell–mediated immunity, and to a lesser extent γδ T cell immunity, has been gleaned. αβ T cells are frequently associated with the adaptive immune response, whereas γδ T cells are considered to exhibit more innate-like features (Vantourout and Hayday, 2013). However, such functional division of these T cell subsets has

Downloaded from http://rupress.org/jem/article-pdf/211/13/2599/1749468/jem_20141764.pdf by guest on 08 February 2026

become blurred. For example, although it was traditionally considered that αβ T cells recognized peptides presented by MHC molecules, innate-like T cells expressing semi-invariant αβTCRs can also recognize distinct nonpeptide-based Ags. Namely, CD1d-restricted type I NKT cells and MR1-restricted MAIT cells, upon activation by lipids and vitamin B metabolites, respectively, rapidly produce an array of cytokines (Rossjohn et al., 2012; Birkinshaw et al., 2014; Gapin, 2014). Furthermore, it is emerging that TCRs can adopt distinct, as well as similar, docking strategies in binding to peptide, lipid, or small molecule metabolites that are bound to their respective Ag-presenting molecules, thereby highlighting the adaptability of the αβTCR scaffold (Bhati et al., 2014).

Whereas most T cells either fall into the $\alpha\beta TCR^+$ or the $\gamma\delta TCR^+$ fraction, the existence of TCR gene rearrangements involving unusual combinations of α, β, γ, and δ chain genes have sporadically been reported in the literature (Hochstenbach and Brenner, 1989; Miossec et al., 1990, 1991; Peyrat et al., 1995; Bowen et al., 2014), although the significance of these unusual gene recombination events, the Ags to which they responded to, and the molecular bases for these interactions are unclear. Here, we have identified populations of $V\delta1^+$ δ/αβ T cells, demonstrating that they are present with a similar frequency to $V\delta1^+$ γδ T cells. Importantly, δ/αβTCRs appear to be functional, capable of transmitting activation signals to the T cells that express them. To understand the molecular bases for how these TCRs recognize Ag, we have focused on two distinct δ/αβTCRs, a CD1d-restricted α-GalCer–reactive δ/αβTCR and an HLA-restricted viral peptide–reactive δ/αβTCR.

We show that the δ/αβTCR architecture resembles that of αβTCRs and γδTCRs and provide a basis for how the Vδ1 chain can pair with the TCR-β chain. The binding of the δ/αβTCR to CD1d was dependent on the nature of the Ag bound, and the mode of recognition was markedly distinct from that of type I NKT TCR–CD1d–α-GalCer docking, more closely resembling that of the γδTCR–CD1d–α-GalCer complex (Uldrich et al., 2013). Indeed, the CDR1δ loop–mediated contacts between the δ/αβTCR and γδTCR were very similar (Uldrich et al., 2013), suggesting a critical role for this region of the TCR in the CD1d restriction of these cells. In contrast, the interactions of the δ/αβTCR with α-GalCer were markedly different from the γδTCR–CD1d–α-GalCer complex. Thus, although the CDR1δ loop appears to represent a focal point for the CD1d-restricted response, the nature of the docking mode is nevertheless fine-tuned by the pairing of the TCR-β or TCR-γ chain and the hypervariable CDR3 loops, in a manner which is strikingly unique to this hybrid TCR. Furthermore, this is the first example of a CD1d–α-GalCer–reactive TCR that does not bind with a parallel docking mode over the F′ pocket of CD1d, a characteristic of all $\alpha\beta TCR^+$ type I NKT cells (Rossjohn et al., 2012).

We also demonstrate how a δ/αβTCR can engage an HLA-I–peptide complex. Notably, the δ/αβTCR docking on CD1d-lipid and HLA-I–peptide differed, despite these two δ/αβTCRs sharing the same $V\delta1\text{-}J\alpha52^+$ chain. Nevertheless, in both cases, the Vδ1 framework region, coupled with the Trp-rich CDR1δ loop, played a prominent role in contacting the respective Ag-presenting molecules. These interactions differed in their positioning on the Ag-binding platforms, thereby highlighting how the same germline-encoded region can play key, yet disparate, roles in binding to polymorphic and monomorphic Ag-presenting molecules.

In summary, our study highlights the existence, and molecular bases for Ag recognition, of T cells that express hybrid TCRs comprised of the Vδ1 variable region rearranged to diverse Jα genes and the Cα constant region and paired to a diverse range of TCR-β chains. These hybrid $\delta/\alpha\beta TCR^+$ T cells are surprisingly abundant in humans and have unique characteristics both at the cellular and molecular level, thus adding a level of diversity that extends beyond the αβ T cell and γδ T cell lineages. Collectively, these findings represent a large conceptual advance in our understanding of T cell–mediated immunity.

MATERIALS AND METHODS

Accession codes. The 9B4 TCR monomer, 9B4 TCR–CD1d–α-GalCer ternary complex, and clone 12 TCR–HLA-B*3501–IPS ternary complex were deposited in the Protein Data Bank (PDB) under the accession codes 4WNQ, 4WO4, and 4QRR, respectively.

Human CD1d–restricted δ/αβ T cell identification and isolation. Healthy human PBMCs were obtained from the Australian Red Cross, ethics approval 13-04VIC-07 (Australian Red Cross) and 1035100.1 (University of Melbourne). PBMCs were isolated using a histopaque-1077 (Sigma-Aldrich) density gradient. $CD3^+$ CD1d–α-GalCer $tetramer^+$ cells were MACS (Miltenyi Biotec) and FACS sort-enriched using a FACSAria III (BD). Enriched $CD3^+$ CD1d–α-GalCer $tetramer^+$ cells were expanded in vitro, essentially as previously described (Uldrich et al., 2013).

Flow cytometry. Enriched $CD3^+$ CD1d–α-GalCer $tetramer^+$ cells were stained with Vδ1 (clone A13 supernatant, which can bind to Vδ1 when incorporated in hybrid Vδ1-Jα-Cα TCR chains, was produced in L. Moretta's laboratory), anti–mouse IgG (clone Poly 4053; BioLegend), 5% normal mouse serum, and then with antibodies specific for αβTCR (clone T10B9.1A-31; BD), CD3ε (clone UCHT1; BD), CD8α (SK1; BD), CD4 (RPA-T4; BD), Vβ11 (C21; Beckman Coulter), CD69 (FN50; BD), γδTCR (11F2; BD), and CD161 (191B8; Miltenyi Biotec). Cells were costained with 7-aminoactinomycin D viability dye (Sigma-Aldrich) and with human CD1d tetramers (produced in-house), as previously described (Uldrich et al., 2013). TCR-Vβ repertoire analysis was performed using a TCR-Vβ repertoire kit (Beckman Coulter). Cells were analyzed using an LSR Fortessa (BD), and data were analyzed using FlowJo software (Tree Star Inc.).

Lipids. Lipids were dissolved in 0.5% Tyloxapol (Sigma-Aldrich) or Tween-sucrose-histidine buffer containing 0.5% vol/vol Tween-20, 57 mg/ml sucrose, and 7.5 mg/ml histidine. Lipids included α-GalCer C24:1 (PBS-44; provided by P. Savage, Brigham Young University, Provo, UT); α-GalCer C26 (Alexis); α-GalCer (C20:2), α-GlcCer C20:2, OCH, 3′,4″-dideoxy-α-GalCer (3′-deoxy-α-GalCer), 4′,4″-dideoxy-α-GalCer (4′-deoxy-α-GalCer; the deoxy analogues were provided by S. Keshipeddy and S. Richardson, University of Connecticut, Storrs, CT; Wun et al., 2011); and sulfatide C24:1 (Avanti Polar Lipids). For CD1d tetramer experiments, lipids were loaded into human CD1d at 3:1 or 6:1 lipid/protein molar ratio by overnight incubation.

Single cell PCR. CD1d–α-GalCer $tetramer\ V\delta1^+\ CD3^+\ \gamma\delta TCR^-$ cells were single cell sorted and cDNA isolated using SuperScript VILO (Invitrogen) as per

Downloaded from http://rupress.org/jem/article-pdf/211/13/2599/1749468/jem_20141764.pdf by guest on 08 February 2026

the manufacturer's instructions. Transcripts encoding for Vδ1 were amplified by two rounds of nested PCR, using Vδ1 external primer 5′-CAAGCCCAGTCATCAGTATCC-3′, Vδ1 internal primer 5′-CAACTTCCCAGCAAAGAGATG-3′, Cα external primer 5′-GACCAGCTTGACATCACAG-3′, and Cα internal primer 5′-TGTTGCTCTTGAAGTCCATAG-3′. Transcripts encoding for the different Vβ genes were identified using multiplex nested PCR as previously described (Wang et al., 2012). PCR fragments were separated using a 1.5% agarose gel and DNA sequenced by Molecular Diagnostics, University of Melbourne.

Generation of cell lines. CD1d-restricted δ/αβTCR$^+$ Jurkat cells (9B4), CD1d-restricted type I NKT TCR$^+$ Jurkat or SKW3 cells (NKT15), and control HLA peptide–specific TCR$^+$ Jurkat cells were generated essentially as previously described (Uldrich et al., 2013). Parental Jurkat-76 cells and SKW3 cells were provided by L. Kjer-Nielsen (University of Melbourne, Parkville, Victoria, Australia).

SPR. SPR experiments were conducted at 25°C on either a BIAcore 3000 (Biacore) or ProteOn XPR36 (Bio-Rad Laboratories) instrument with HBS buffer (10 mM Hepes, pH 7.4, 150 mM NaCl, and 0.005% surfactant P-20). In some instances the HBS buffer was supplemented with 1% bovine serum albumin to prevent nonspecific binding. The human αβTCR–specific mAb (clone 12H8; Borg et al., 2005) or streptavidin was coupled to CM5 or GLC chips with standard amine coupling, respectively. Experiments were conducted as previously described (Gras et al., 2009; Pellicci et al., 2009). BIAevaluation version 3.1 (Biacore) or ProteOn Manager version 2.1 (Bio-Rad Laboratories) software was used for data analysis with 1:1 Langmuir binding model. The equilibrium data were analyzed using Prism (GraphPad Software).

Cloning and expression of TCRs, human CD1d, and HLA. Soluble TCRs, including CD1d-restricted δ/αβTCR (9B4), type I NKT TCR (NKT15), and HLA-B*35–IPS (clone 12), were generated as previously described (Kjer-Nielsen et al., 2006). In brief, gene fragments encoding the TCR ectodomains were cloned into pET30 expression vector (EMD Millipore) and expressed in BL-21 *Escherichia coli* cells. Inclusion body protein was prepared and refolded similar to that previously described in Clements et al. (2002) except in the presence of 5 M urea. Human CD1d with and without a Bir-A tag were expressed and purified as previously described (Borg et al., 2007; Uldrich et al., 2013). Soluble pHLA-B*35:01 was prepared as described previously (Gras et al., 2010). The 9B4 TCR–CD1d–α-GalCer and clone 12 TCR–HLA-B*35:01–IPS ternary complexes were purified by gel filtration from mixtures of the respective monomers.

Structure determination. Solutions of the 9B4 TCR monomer (at 5 mg/ml in 10 mM Tris-HCl, pH 8.0, and 150 mM NaCl) and 9B4 TCR-CD1d–α-GalCer ternary complex (at 10 mg/ml in 10 mM Tris-HCl, pH 8.7, and 150 mM NaCl) were crystallized at 20°C in 27% PEG 1500 plus 0.1 M sodium malonate/imidazole/borate buffer (at a 2:3:3 molar ratio), pH 8.1, in hanging drops and 3% PEG 3350 in sitting drops, respectively. Plate-like crystals of the clone 12 TCR–HLA-B*35:01–IPS complex (at 4 mg/ml) were grown at 20°C with 0.3 M potassium thiocyanate, 24% PEG 3350, 2% ethylene glycol, 10 mM L-Proline, and 10 mM spermidine. Crystals of 9B4 monomer and CD1d ternary complex were flash frozen in well solution plus 2-methyl-2,4-pentanediol, whereas the clone 12–IPS ternary complex crystals were soaked in mother liquor with 25% PEG 3350 and 5% (wt/vol) ethylene glycol as cryoprotectant and then flash frozen in liquid nitrogen. Data were collected at 100 K on the MX1 and MX2 beam lines at the Australian Synchrotron (Melbourne). Data were integrated using iMosflm or XDS (Kabsch, 2010) software and scaled using the SCALA package of the CCP4 suite. The 9B4 TCR–CD1d–α-GalCer ternary complex was solved by molecular replacement using PHASER with three separate search ensembles: CD1d without α-GalCer, TCR minus the Vα domain and CDRβ loops, and Vδ1 minus the CDRδ loops (derived from PDB codes 1ZT4 [Koch et al., 2005], 4DZB [Reantragoon et al., 2012], and 4LFH [Uldrich et al., 2013], respectively). The structure of unligated 9B4 TCR was solved by molecular replacement using the refined 9B4 TCR structure derived from the ternary complex. There were two TCR monomers in each asymmetric unit with an rmsd of 0.1 Å over 432 Cα atoms; thus, structural analysis was restricted to one TCR molecule. The clone 12 TCR–HLA-B*35:01–IPS complex was solved as above, using the 9C2 TCR (Uldrich et al., 2013) and HLA-B*3501 without the peptide (PDB code 3LKN [Gras et al., 2010]) as search models. All structures were refined into the experimental maps by iterative rounds of model building using COOT (Emsley et al., 2010) and refinement with BUSTER (Bricogne et al., 2011). The electron density at the Ag interfaces was clear, with unbiased electron density for IPS peptide, the α-GalCer headgroup, and all CDR loops of the 9B4 and clone 12 TCR. Structural models were validated at the Research Collaboratory for Structural Bioinformatics Protein Data Bank Data Validation and Deposition Services website, and molecular illustrations were generated using the PyMOL package (DeLano, 2002). Domain superpositions and rmsd calculations were based on Cα atoms.

Online supplemental material. Table S1 shows data collection and refinement statistics. Table S2 shows 9B4 δ/αβTCR contacts with CD1d–α-GalCer. Table S3 shows clone 12 δ/αβTCR contacts with HLA-B*35:01–IPS. Online supplemental material is available at http://www.jem.org/cgi/content/full/jem.20141764/DC1.

We thank John Waddington and Marcin Ciula at the University of Melbourne (Parkville, Victoria, Australia) for assistance with protein production, the staff at the Australian Synchrotron for assistance with data collection, and the Macromolecular Crystallization Facility at Monash University for technical assistance. We thank Dr. Richard Birkinshaw for assistance with data collection and integration, Professor Paul Savage for kindly providing the PBS-44 α-GalCer analogue, and Santosh Keshipeddy and Stewart Richardson for the deoxy-α-GalCer analogues.

This work was supported by the Australian Research Council (ARC; DP110104124, CE140100011, and LE110100106), the National Health and Medical Research Council of Australia (NHMRC; #1013667), the Cancer Council of Victoria (#1042866), and National Institutes of Health RO1 grant (GM 087136). D.G. Pellicci is supported by an NHMRC Biomedical fellowship, A.P. Uldrich by an ARC Future Fellowship (FT140100278), S. Gras by an ARC Future Fellowship (FT120100416), D.I. Godfrey by an NHMRC Senior Principal Research Fellowship (#1020770), and J. Rossjohn by an NHMRC Australia Fellowship (AF50).

The authors declare no competing financial interests.

Author contributions: D.G. Pellicci and A.P. Uldrich identified and performed cellular and molecular characterization of δ/αβ T cells. S.B.G. Eckle, R. de Boer, D.G. Pellicci, A.P. Uldrich, S. Gras, and E. Chabrol produced TCR protein complexes for crystallographic experiments. A.P. Uldrich, J. Le Nours, E. Chabrol, and S. Gras solved the crystal structures. E. Chabrol, M.H.M. Heemskerk, R. de Boer, S.B.G. Eckle, and J. McCluskey undertook or supervised experiments on the MHC-restricted δ/αβTCR. A.P. Uldrich, D.G. Pellicci, and S. Gras undertook SPR investigations, wrote the paper, and generated figures. D.G. Pellicci, A.P. Uldrich, F. Ross, K. McPherson, and R.T. Lim performed cell-based experiments, including glycolipid specificity and functional studies. L. Moretta, A.R. Howell, and G. Besra provided reagents that were crucial to this study. J. Rossjohn and D.I. Godfrey were joint senior authors: they co-led the investigation, devised the project, and wrote the paper.

Submitted: 10 September 2014
Accepted: 5 November 2014

REFERENCES

Amir, A.L., D.M. van der Steen, R.S. Hagedoorn, M.G. Kester, C.A. van Bergen, J.W. Drijfhout, A.H. de Ru, J.H. Falkenburg, P.A. van Veelen, and M.H. Heemskerk. 2011. Allo-HLA-reactive T cells inducing graft-versus-host disease are single peptide specific. *Blood.* 118:6733–6742. http://dx.doi.org/10.1182/blood-2011-05-354787

Bhati, M., D.K. Cole, J. McCluskey, A.K. Sewell, and J. Rossjohn. 2014. The versatility of the αβ T-cell antigen receptor. *Protein Sci.* 23:260–272. http://dx.doi.org/10.1002/pro.2412

Birkinshaw, R.W., L. Kjer-Nielsen, S.B. Eckle, J. McCluskey, and J. Rossjohn. 2014. MAITs, MR1 and vitamin B metabolites. *Curr. Opin. Immunol.* 26:7–13. http://dx.doi.org/10.1016/j.coi.2013.09.007

Downloaded from http://rupress.org/jem/article-pdf/211/13/2599/1749468/jem_20141764.pdf by guest on 08 February 2026

Borg, N.A., L.K. Ely, T. Beddoe, W.A. Macdonald, H.H. Reid, C.S. Clements, A.W. Purcell, L. Kjer-Nielsen, J.J. Miles, S.R. Burrows, et al. 2005. The CDR3 regions of an immunodominant T cell receptor dictate the 'energetic landscape' of peptide-MHC recognition. *Nat. Immunol.* 6:171–180. http://dx.doi.org/10.1038/ni1155

Borg, N.A., K.S. Wun, L. Kjer-Nielsen, M.C. Wilce, D.G. Pellicci, R. Koh, G.S. Besra, M. Bharadwaj, D.I. Godfrey, J. McCluskey, and J. Rossjohn. 2007. CD1d-lipid-antigen recognition by the semi-invariant NKT T-cell receptor. *Nature*. 448:44–49. http://dx.doi.org/10.1038/nature05907

Born, W.K., M. Kemal Aydintug, and R.L. O'Brien. 2013. Diversity of γδ T-cell antigens. *Cell. Mol. Immunol.* 10:13–20. http://dx.doi.org/10.1038/cmi.2012.45

Bowen, S., P. Sun, F. Livak, S. Sharrow, and R.J. Hodes. 2014. A novel T cell subset with trans-rearranged Vγ-Cβ TCRs shows Vβ expression is dispensable for lineage choice and MHC restriction. *J. Immunol.* 192:169–177. http://dx.doi.org/10.4049/jimmunol.1302398

Bricogne, G., E. Blanc, M. Brandl, C. Flensburg, P. Keller, W. Paciorek, P. Roversi, A. Sharff, O.S. Smart, C. Vonrhein, and T.O. Womack. 2011. autoBUSTER, Version 1.6.0. Global Phasing Ltd, Cambridge, UK. Available at: https://www.globalphasing.com/buster/ (accessed June 29, 2014).

Brigl, M., and M.B. Brenner. 2004. CD1: antigen presentation and T cell function. *Annu. Rev. Immunol.* 22:817–890. http://dx.doi.org/10.1146/annurev.immunol.22.012703.104608

Brossay, L., O. Naidenko, N. Burdin, J. Matsuda, T. Sakai, and M. Kronenberg. 1998. Structural requirements for galactosylceramide recognition by CD1-restricted NK T cells. *J. Immunol.* 161:5124–5128.

Burrows, S.R., Z. Chen, J.K. Archbold, F.E. Tynan, T. Beddoe, L. Kjer-Nielsen, J.J. Miles, R. Khanna, D.J. Moss, Y.C. Liu, et al. 2010. Hard wiring of T cell receptor specificity for the major histocompatibility complex is underpinned by TCR adaptability. *Proc. Natl. Acad. Sci. USA.* 107:10608–10613. http://dx.doi.org/10.1073/pnas.1004926107

Ciofani, M., and J.C. Zúñiga-Pflücker. 2010. Determining γδ versus αß T cell development. *Nat. Rev. Immunol.* 10:657–663.

Clements, C.S., L. Kjer-Nielsen, W.A. MacDonald, A.G. Brooks, A.W. Purcell, J. McCluskey, and J. Rossjohn. 2002. The production, purification and crystallization of a soluble heterodimeric form of a highly selected T-cell receptor in its unliganded and liganded state. *Acta Crystallogr. D Biol. Crystallogr.* 58:2131–2134. http://dx.doi.org/10.1107/S0907444902015482

Corbett, A.J., S.B. Eckle, R.W. Birkinshaw, L. Liu, O. Patel, J. Mahony, Z. Chen, R. Reantragoon, B. Meehan, H. Cao, et al. 2014. T-cell activation by transitory neo-antigens derived from distinct microbial pathways. *Nature*. 509:361–365. http://dx.doi.org/10.1038/nature13160

DeLano, W.L. 2002. The PyMOL Molecular Graphics System. Available at: http://www.pymol.org (accessed June 29, 2014).

Eckle, S.B., R.W. Birkinshaw, L. Kostenko, A.J. Corbett, H.E. McWilliam, R. Reantragoon, Z. Chen, N.A. Gherardin, T. Beddoe, L. Liu, et al. 2014. A molecular basis underpinning the T cell receptor heterogeneity of mucosal-associated invariant T cells. *J. Exp. Med.* 211:1585–1600. http://dx.doi.org/10.1084/jem.20140484

Emsley, P., B. Lohkamp, W.G. Scott, and K. Cowtan. 2010. Features and development of Coot. *Acta Crystallogr. D Biol. Crystallogr.* 66:486–501. http://dx.doi.org/10.1107/S0907444910007493

Gapin, L. 2014. Check MAIT. *J. Immunol.* 192:4475–4480. http://dx.doi.org/10.4049/jimmunol.1400119

Girardi, E., and D.M. Zajonc. 2012. Molecular basis of lipid antigen presentation by CD1d and recognition by natural killer T cells. *Immunol. Rev.* 250:167–179. http://dx.doi.org/10.1111/j.1600-065X.2012.01166.x

Girardi, E., I. Maricic, J. Wang, T.T. Mac, P. Iyer, V. Kumar, and D.M. Zajonc. 2012. Type II natural killer T cells use features of both innate-like and conventional T cells to recognize sulfatide self antigens. *Nat. Immunol.* 13:851–856. http://dx.doi.org/10.1038/ni.2371

Godfrey, D.I., J. McCluskey, and J. Rossjohn. 2005. CD1d antigen presentation: treats for NKT cells. *Nat. Immunol.* 6:754–756. http://dx.doi.org/10.1038/ni0805-754

Godfrey, D.I., J. Rossjohn, and J. McCluskey. 2008. The fidelity, occasional promiscuity, and versatility of T cell receptor recognition. *Immunity.* 28:304–314. http://dx.doi.org/10.1016/j.immuni.2008.02.004

Gras, S., S.R. Burrows, L. Kjer-Nielsen, C.S. Clements, Y.C. Liu, L.C. Sullivan, M.J. Bell, A.G. Brooks, A.W. Purcell, J. McCluskey, and J. Rossjohn. 2009. The shaping of T cell receptor recognition by self-tolerance. *Immunity.* 30:193–203. http://dx.doi.org/10.1016/j.immuni.2008.11.011

Gras, S., Z. Chen, J.J. Miles, Y.C. Liu, M.J. Bell, L.C. Sullivan, L. Kjer-Nielsen, R.M. Brennan, J.M. Burrows, M.A. Neller, et al. 2010. Allelic polymorphism in the T cell receptor and its impact on immune responses. *J. Exp. Med.* 207:1555–1567. http://dx.doi.org/10.1084/jem.20100603

Gras, S., S.R. Burrows, S.J. Turner, A.K. Sewell, J. McCluskey, and J. Rossjohn. 2012. A structural voyage toward an understanding of the MHC-I-restricted immune response: lessons learned and much to be learned. *Immunol. Rev.* 250:61–81. http://dx.doi.org/10.1111/j.1600-065X.2012.01159.x

Hedrick, S.M., D.I. Cohen, E.A. Nielsen, and M.M. Davis. 1984. Isolation of cDNA clones encoding T cell-specific membrane-associated proteins. *Nature*. 308:149–153. http://dx.doi.org/10.1038/308149a0

Hochstenbach, F., and M.B. Brenner. 1989. T-cell receptor δ-chain can substitute for α to form a βδ heterodimer. *Nature*. 340:562–565. http://dx.doi.org/10.1038/340562a0

Kabsch, W. 2010. Xds. *Acta Crystallogr. D Biol. Crystallogr.* 66:125–132. http://dx.doi.org/10.1107/S0907444909047337

Kjer-Nielsen, L., N.A. Borg, D.G. Pellicci, T. Beddoe, L. Kostenko, C.S. Clements, N.A. Williamson, M.J. Smyth, G.S. Besra, H.H. Reid, et al. 2006. A structural basis for selection and cross-species reactivity of the semi-invariant NKT cell receptor in CD1d/glycolipid recognition. *J. Exp. Med.* 203:661–673. http://dx.doi.org/10.1084/jem.20051777

Kjer-Nielsen, L., O. Patel, A.J. Corbett, J. Le Nours, B. Meehan, L. Liu, M. Bhati, Z. Chen, L. Kostenko, R. Reantragoon, et al. 2012. MR1 presents microbial vitamin B metabolites to MAIT cells. *Nature*. 491:717–723.

Koch, M., V.S. Stronge, D. Shepherd, S.D. Gadola, B. Mathew, G. Ritter, A.R. Fersht, G.S. Besra, R.R. Schmidt, E.Y. Jones, and V. Cerundolo. 2005. The crystal structure of human CD1d with and without α-galactosylceramide. *Nat. Immunol.* 6:819–826. http://dx.doi.org/10.1038/ni1225

Lefranc, M.P., and T.H. Rabbitts. 1990. Genetic organization of the human T-cell receptor γ and δ loci. *Res. Immunol.* 141:565–577. http://dx.doi.org/10.1016/0923-2494(90)90058-7

Luoma, A.M., C.D. Castro, T. Mayassi, L.A. Bembinster, L. Bai, D. Picard, B. Anderson, L. Scharf, J.E. Kung, L.V. Sibener, et al. 2013. Crystal structure of Vδ1 T cell receptor in complex with CD1d-sulfatide shows MHC-like recognition of a self-lipid by human γδ T cells. *Immunity.* 39:1032–1042. http://dx.doi.org/10.1016/j.immuni.2013.11.001

Mangan, B.A., M.R. Dunne, V.P. O'Reilly, P.J. Dunne, M.A. Exley, D. O'Shea, E. Scotet, A.E. Hogan, and D.G. Doherty. 2013. Cutting edge: CD1d restriction and Th1/Th2/Th17 cytokine secretion by human Vδ3 T cells. *J. Immunol.* 191:30–34. http://dx.doi.org/10.4049/jimmunol.1300121

Matulis, G., J.P. Sanderson, N.M. Lissin, M.B. Asparuhova, G.R. Bommineni, D. Schümperli, R.R. Schmidt, P.M. Villiger, B.K. Jakobsen, and S.D. Gadola. 2010. Innate-like control of human iNKT cell autoreactivity via the hypervariable CDR3β loop. *PLoS Biol.* 8:e1000402. http://dx.doi.org/10.1371/journal.pbio.1000402

Miossec, C., F. Faure, L. Ferradini, S. Roman-Roman, S. Jitsukawa, S. Ferrini, A. Moretta, F. Triebel, and T. Hercend. 1990. Further analysis of the T cell receptor gamma/delta+ peripheral lymphocyte subset. The V delta 1 gene segment is expressed with either C alpha or C delta. *J. Exp. Med.* 171:1171–1188. http://dx.doi.org/10.1084/jem.171.4.1171

Miossec, C., A. Caignard, L. Ferradini, S. Roman-Roman, F. Faure, H. Michalaki, F. Triebel, and T. Hercend. 1991. Molecular characterization of human T cell receptor α chains including a Vδ1-encoded variable segment. *Eur. J. Immunol.* 21:1061–1064. http://dx.doi.org/10.1002/eji.1830210430

O'Brien, R.L., C.L. Roark, N. Jin, M.K. Aydintug, J.D. French, J.L. Chain, J.M. Wands, M. Johnston, and W.K. Born. 2007. γδ T-cell receptors: functional correlations. *Immunol. Rev.* 215:77–88. http://dx.doi.org/10.1111/j.1600-065X.2006.00477.x

Downloaded from http://rupress.org/jem/article-pdf/211/13/2599/1749468/jem_20141764.pdf by guest on 08 February 2026

Patel, O., D.G. Pellicci, S. Gras, M.L. Sandoval-Romero, A.P. Uldrich, T. Mallevaey, A.J. Clarke, J. Le Nours, A. Theodossis, S.L. Cardell, et al. 2012. Recognition of CD1d-sulfatide mediated by a type II natural killer T cell antigen receptor. *Nat. Immunol.* 13:857–863. http://dx.doi.org/10.1038/ni.2372

Patel, O., L. Kjer-Nielsen, J. Le Nours, S.B. Eckle, R. Birkinshaw, T. Beddoe, A.J. Corbett, L. Liu, J.J. Miles, B. Meehan, et al. 2013. Recognition of vitamin B metabolites by mucosal-associated invariant T cells. *Nat. Commun.* 4:2142. http://dx.doi.org/10.1038/ncomms3142

Pellicci, D.G., O. Patel, L. Kjer-Nielsen, S.S. Pang, L.C. Sullivan, K. Kyparissoudis, A.G. Brooks, H.H. Reid, S. Gras, I.S. Lucet, et al. 2009. Differential recognition of CD1d-α-galactosyl ceramide by the Vβ8.2 and Vβ7 semi-invariant NKT T cell receptors. *Immunity.* 31:47–59. http://dx.doi.org/10.1016/j.immuni.2009.04.018

Peyrat, M.A., F. Davodeau, I. Houde, F. Romagné, A. Necker, C. Leget, J.P. Cervoni, N. Cerf-Bensussan, H. Vié, M. Bonneville, et al. 1995. Repertoire analysis of human peripheral blood lymphocytes using a human V delta 3 region-specific monoclonal antibody. Characterization of dual T cell receptor (TCR) delta-chain expressors and alpha beta T cells expressing V delta 3J alpha C alpha-encoded TCR chains. *J. Immunol.* 155:3060–3067.

Reantragoon, R., L. Kjer-Nielsen, O. Patel, Z. Chen, P.T. Illing, M. Bhati, L. Kostenko, M. Bharadwaj, B. Meehan, T.H. Hansen, et al. 2012. Structural insight into MR1-mediated recognition of the mucosal associated invariant T cell receptor. *J. Exp. Med.* 209:761–774. http://dx.doi.org/10.1084/jem.20112095

Rossjohn, J., D.G. Pellicci, O. Patel, L. Gapin, and D.I. Godfrey. 2012. Recognition of CD1d-restricted antigens by natural killer T cells. *Nat. Rev. Immunol.* 12:845–857. http://dx.doi.org/10.1038/nri3328

Sandstrom, A., C.M. Peigné, A. Léger, J.E. Crooks, F. Konczak, M.C. Gesnel, R. Breathnach, M. Bonneville, E. Scotet, and E.J. Adams. 2014. The intracellular B30.2 domain of butyrophilin 3A1 binds phosphoantigens to mediate activation of human Vγ9Vδ2 T cells. *Immunity.* 40:490–500. http://dx.doi.org/10.1016/j.immuni.2014.03.003

Scott-Browne, J.P., J.L. Matsuda, T. Mallevaey, J. White, N.A. Borg, J. McCluskey, J. Rossjohn, J. Kappler, P. Marrack, and L. Gapin. 2007. Germline-encoded recognition of diverse glycolipids by natural killer T cells. *Nat. Immunol.* 8:1105–1113. http://dx.doi.org/10.1038/ni1510

Turner, S.J., P.C. Doherty, J. McCluskey, and J. Rossjohn. 2006. Structural determinants of T-cell receptor bias in immunity. *Nat. Rev. Immunol.* 6:883–894. http://dx.doi.org/10.1038/nri1977

Uldrich, A.P., J. Le Nours, D.G. Pellicci, N.A. Gherardin, K.G. McPherson, R.T. Lim, O. Patel, T. Beddoe, S. Gras, J. Rossjohn, and D.I. Godfrey. 2013. CD1d-lipid antigen recognition by the γδ TCR. *Nat. Immunol.* 14:1137–1145. http://dx.doi.org/10.1038/ni.2713

Vantourout, P., and A. Hayday. 2013. Six-of-the-best: unique contributions of γδ T cells to immunology. *Nat. Rev. Immunol.* 13:88–100. http://dx.doi.org/10.1038/nri3384

Vavassori, S., A. Kumar, G.S. Wan, G.S. Ramanjaneyulu, M. Cavallari, S. El Daker, T. Beddoe, A. Theodossis, N.K. Williams, E. Gostick, et al. 2013. Butyrophilin 3A1 binds phosphorylated antigens and stimulates human γδ T cells. *Nat. Immunol.* 14:908–916. http://dx.doi.org/10.1038/ni.2665

Wang, G.C., P. Dash, J.A. McCullers, P.C. Doherty, and P.G. Thomas. 2012. T cell receptor αβ diversity inversely correlates with pathogen-specific antibody levels in human cytomegalovirus infection. *Sci. Transl. Med.* 4:128ra42. http://dx.doi.org/10.1126/scitranslmed.3003647

Wun, K.S., G. Cameron, O. Patel, S.S. Pang, D.G. Pellicci, L.C. Sullivan, S. Keshipeddy, M.H. Young, A.P. Uldrich, M.S. Thakur, et al. 2011. A molecular basis for the exquisite CD1d-restricted antigen specificity and functional responses of natural killer T cells. *Immunity.* 34:327–339. http://dx.doi.org/10.1016/j.immuni.2011.02.001

Wun, K.S., F. Ross, O. Patel, G.S. Besra, S.A. Porcelli, S.K. Richardson, S. Keshipeddy, A.R. Howell, D.I. Godfrey, and J. Rossjohn. 2012. Human and mouse type I natural killer T cell antigen receptors exhibit different fine specificities for CD1d-antigen complex. *J. Biol. Chem.* 287:39139–39148. http://dx.doi.org/10.1074/jbc.M112.412320

Xiong, N., and D.H. Raulet. 2007. Development and selection of γδ T cells. *Immunol. Rev.* 215:15–31. http://dx.doi.org/10.1111/j.1600-065X.2006.00478.x

Downloaded from http://rupress.org/jem/article-pdf/211/13/2599/1749468/jem_20141764.pdf by guest on 08 February 2026